Characterization of Rag Layer Formed by Actual Crude Oil, Synthetic Microcrystalline Wax and Synthetic Macrocrystalline Wax

By

Muhamad Faris Ashraf bin Md Nasser
14974

Dissertation submitted in partial fulfilment of
the requirements for the
Bachelor of Engineering (Hons.)
(Mechanical)

SEPTEMBER 2014

Universiti Teknologi PETRONAS
Bandar Seri Iskandar
31750
Perak Darul Ridzuan

CERTIFICATION OF APPROVAL

Characterization of Rag Layer Formed by Actual Crude Oil, Synthetic Microcrystalline Wax and Synthetic Macrocrystalline Wax

By

Muhamad Faris Ashraf bin Md Nasser

14974

Dissertation submitted in partial fulfilment of
the requirements for the
Bachelor of Engineering (Hons.)
(Mechanical)

SEPTEMBER 2014

Approved by:

_____

Azuraien Bt. Japper @ Jaafar

Universiti Teknologi PETRONAS
Bandar Seri Iskandar
31750 Tronoh
Perak Darul Ridzuan

CERTIFICATION OF ORIGINALITY

This is to certify that I am responsible for the work submitted in this project, that the original work is my own except as specified in the references and acknowledgements, and that the original work contained herein have not been undertaken or done by unspecified sources or persons.

_____

MUHAMAD FARIS ASHRAF BIN MD NASSER

ACKNOWLEDGEMENT

All praises to Allah for guidance and blessings for giving an opportunity for the author to complete this Final Year Project as part of requirements for Bachelor of Engineering (Hons.) in Mechanical Engineering at Universiti Teknologi PETRONAS (UTP).

The author would like to express his most appreciation to his supervisor for this project, Dr. Azuraien Japper @ Jaafar for her continuous guidance and support provided throughout the progression of his project. Many thanks to Abdulrahman Yousif for his advice and support in making this final year project a success.

This acknowledgement would not be complete without giving credit to UTP, especially the team at the Flow Assurance Lab at the Mechanical Engineering Department which has equipped students with essential skills for self-learning.

ABSTRACT

The mechanical characteristics of crude oil has several importance, especially during the period of extraction and separation of crude oil. It gives an insight to the behaviour bnof the crude oil inside the pipeline and the potential problems that may happen. In addition to that, the presence of rag layer, or emulsion pad, which is due to the mixture between the crude oil and water can be very disruptive in the separation process. Thus, it is imperative to know the similarities and differences between the crude oils and its rag layers so as to minimize the disruption in the process. To resolve the rag layer problem, it is important to understand the properties and characteristics of the rag layer including the role of solid particles to the emulsion layer stability. Many studies have been conducted on the effects of asphaltenes and resins but none on the effects of micro and macro crystalline wax.

TABLE OF CONTENTS

LIST OF FIGURES

LIST OF TABLES

CHAPTER 1

INTRODUCTION

1.1. Background

Crude oil extraction has never been easy as many factors are taken into consideration, especially on the characteristics of the crude oil itself. Due to the slow coalescence mechanics, an emulsion pad, also known as rag layer, is formed based on the accumulation of material. The rag layer is known to be disruptive during the separation process due to its hydrophobic nature. In addition to that, the rag layer is known to be a set of complex multiple emulsion making it hard to be separated.

Studies on rag layer have been progressing in the previous years. However, it remains a problem in the oil and gas industry, especially in extracting heavy crude oils with API higher than 20. In unfavourable conditions, the rag layer may be thick enough that it goes into the oil and water outlet stream and cause corrosion or fouling in downstream processes. When introduced into the water stream, additional treatment are needed as the oil recovery rate has been reduced. While this is often observed on froth treatment processes, it also occurs on conventional and heavy oil separation processes. (Saadatmand, et al., 2008)

A study on the characteristics of rag layer, particularly those present in the Malaysian crude oils is imperative to tackle the rag layer problem. Therefore, this study on rag layer is hoped to contribute towards the industry in the future.

1.2. Problem Statement

The presence of rag layer in crude oil has long been one of the major difficulties in the process of extraction and production of crude oil, particularly during separation. Understanding or characterising the rag layer is important to ensure that the problems caused by the rag layer can be minimized so that smooth extraction across the line can be achieved. Many studies have also been conducted on the effects of asphaltenes and resins on rag layer but none on the effects of micro and macro crystalline wax.

1.3. Objectives and Scope of Study

The objectives of this project is to:

1. Characterize the rag layers produced by two different crude oils, which are Sample A and Sample B, and two synthetic wax solutions or artificial waxy crude oils, namely synthetic microcrystalline wax solution and macrocrystalline wax solution, each with artificially produced water.
2. Using mechanical analytical methods including the use of a rheometer, pour point device, differential scanning calorimeter, goniometer, and a cross-polar microscope to characterize the rag layers.

The scope of study will focus on the rag layer that is produced from 70% crude oil (actual or artificial crude oils) with 30% of water as this ratio was found to be the common emulsion ratio found in offshore extraction as well as being the emulsion ratio that produces the most significant amount of rag layer based on a study conducted in the same flow assurance lab.

CHAPTER 2

LITERATURE REVIEW/THEORY

2.1. Waxy Crude Oil Emulsion

2.1.1. Overview & Stabilizing Agent

Emulsion on waxy crude oil refers to the water-in-oil condition that is usually found after oil spills and is often considered to be the complicating factor of an oil spill cleanup process. This is due to the fact that the physical properties and characteristics of the oil differ drastically due to emulsion (Fingas & Fieldhouse, 2008). Under such condition, the stable emulsion contained between 65% to 85% water, depending on its stability, making clean up harder as the volume can be up to five times more than the original amount of oil spilled. Emulsions could also be created when hydrocarbon liquid is produced together with water and is stabilized. In any cases, from the same study done by Fingas and Fieldhouse (2008), it was stated that the viscosity of the mixture of oil and water increases as much as 500 times more than the individual samples making the combination a heavy, semi-solid material. This does not take into account the rag layer, which consists of a sizable amount of water inside.

Based on the study done by Berridge et.al (1968), it was found that asphaltenes was the main contributor in the emulsions found in oil spills. In short, the emulsions were stabilized by the formation of asphaltenes layers around the water droplets. While resins also played a part in forming emulsions, it did not form stabilized water-in-oil emulsions. However, it may have aided the asphaltenes to stabilize the emulsions by acting as a solvent.

It was also found on the same study that the aromaticity of the crude to be a major influence in the appearance of emulsions. The availability of asphaltenes and solvating resins were important as the former worked best in forming emulsions when the resins were at the point of incipient precipitation.

2.1.2. Treating Emulsions

There are many ways of treating water-in-oil emulsions, as there were plenty of research and experiments conducted on the subject. These include heating, free water separation, the use of insulated vessels, chemical demulsifiers, and agitation amongst many others.

2.2. Wax Appearance Temperature (W.A.T)

Wax appearance temperature is the condition of the crude when it reaches a temperature and pressure that is low enough for wax molecules to form. Any decrease in temperature will increase the viscosity of the crude oil due to the presence of wax crystals.

In addition to that, further decrease in temperature and pressure may also result in the pour point, which is the lowest temperature on which a sample of the fluid shows flow characteristics under defined condition.

This then would result significant increase of high-pressure drop and cause tremendous problems during shutdown. The worst case would be that the wax would gel up completely and has high gel strength. If the latter is too high, the line may not be restarted due to the high stress it would pose on the line.

Inhibitors in the form of wax crystal modifiers and dispersants are commonly used to reduce the transportation problem due to the presence of wax. In a way, these inhibitors ensure that the wax crystals stay dispersed as separate particles and not lumped together. In return, these substances will not be deposited on the wall of the pipe but flow together with the liquid hydrocarbon.

2.3. Emulsion Stability Mechanism

2.3.1. Flocculation & Coalescence

Flocculation is the first step in the demulsification process. The emulsion droplets clump together to form aggregates. The particles do not yet fuse with each other although they may appear to be touching one another at certain points. Coalescence only happens if the emulsifying film is very weak. The rate of flocculation depends on the following:

- Amount of water in emulsion
- Temperature of the emulsion
- Viscosity of the oil
- Density between water and oil.

Coalescence refers to the second step of the demulsification process. Here, the droplets that have flocculated fuse with each other to form a larger drop. It is an irreversible process that then leads to the reduction of oil droplets before reaching full demulsification. The following factor affects the coalescence process:

- Rate of flocculation
- Absence of mechanically strong emulsion films
- High interfacial tension
- High water cut
- Low interfacial viscosity
- Presence of chemical demulsifiers

2.3.2. Creaming & Sedimentation

Both creaming and sedimentation happens due to the difference in gravity between the droplets and the crude oil. Sedimentation happens when the water droplets settle down due to the higher density while creaming happens due to the lower density. The two processes happen due to the difference in density although it may not result in the breakage of the emulsion.

An emulsion pad or a rag layer will be formed when the emulsion droplets accumulate at the oil/water interface. This may then cause several problems such as:

- Increase in residual oil in treated water
- Increase in BS&W of the treated oil
- Occupies more space in separation tank
- Acts as barrier for water droplets/solids to settle

The rag layer are often caused or made worse by:

- Use of ineffective demulsifier
- Insufficient demulsifier
- Low temperature
- Presence of accumulating solid

Therefore, the rag layer needs to be treated so that it will not cause further operational problems. Figure 1 shows the emulsion stability mechanism in general and the stages that it goes.

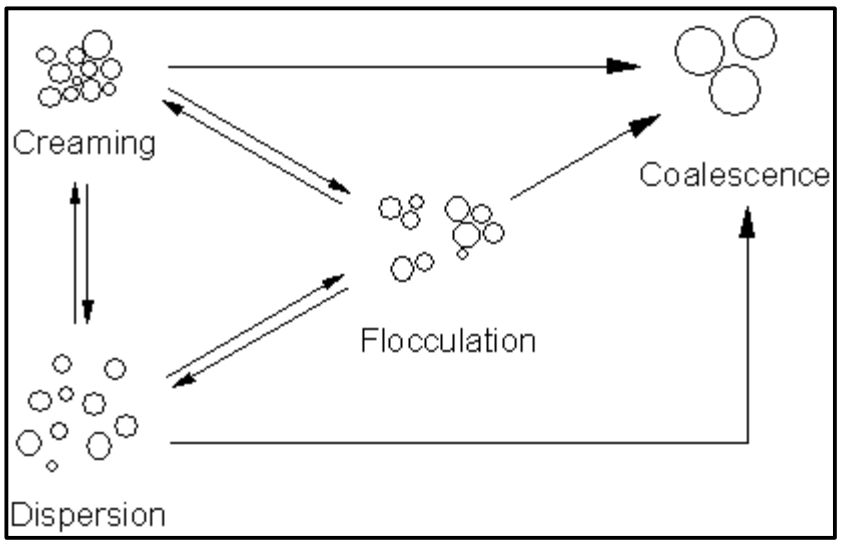

Figure 1 – Emulsion Stability Mechanism (Wabel, 1998)

2.3.3. Ostwald Ripening

Jiao and Burgess (2003), mentioned that the Ostwald ripening phenomena occurs when then smaller particles in a solution dissolves and then deposits into the larger particles. The resulting particle will be more thermodynamically stable. In the case of crude oil emulsion, the particles described are in the form of droplets.

This happens usually because the surface of the smaller droplets is more energetically unstable as compared with the bigger droplets. As such, the unstable droplets shrink over time and increase the number of free molecules in the solution. Once the solution is supersaturated, the free molecules will then be deposited at the larger droplets and gets absorbed by it.

Ostwald ripening is often found in the oil-in-water emulsions where the oil molecule will diffuse through the aqueous state and join the larger oil droplets (Particle Sizing System, 2012). Figure 2 below shows the diffusion process in Ostwald ripening.

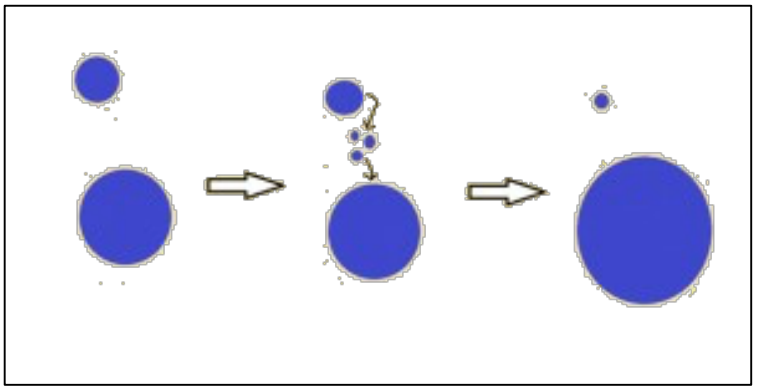

Figure 2 – Ostwald Ripening (Particle Sizing System, 2012)

2.4. Demulsification Methods

Emulsions can be demulsified through various methods, namely through a chemical demulsifier, by heating as well as through aerations.

2.4.1. Chemical Demulsifier

The most popular method used to treat emulsion was through the use of chemical demulsifiers (PetroWiki, 2014). These dehydration chemicals were used to destabilize crude-oil emulsions stabilizing agents, namely asphaltenes, resins and other hydrocarbons.

To demulsify, the chemicals are injected into the emulsion and must be mixed and dispersed through all possible areas in the emulsion so that all of the protective films can be removed. The emulsion needs to be agitated and then settles due to gravity. This then separates water and oil.

However, in the case of low flow rates, injection may not be recommended. As such, the use of injection quill, chemical distributor or a static mixer is the better option.

Bottle tests are often done prior to well testing so that a set of the best demulsifiers can be chosen before application. Samples of the emulsion are to be taken to centrifuge tubes and different demulsifiers are tested at different amounts. Water-dropout data are then taken and analyzed to see which chemical demulsifier works best with the particular emulsion.

Selecting the best demulsifier also requires testing at different temperature, concentrations and water cuts. Appearance of the emulsion, clarity of the water, sediments in the water, as well as the presence of a rag layer need to be assessed.

Once the bottle tests are conducted, a few demulsifiers that has been selected will be taken to the field for further test. The chemicals are then injected at various concentrations, operating temperatures, and settling time. The common range of concentration used is often between 10 and 50ppm (PetroWiki, 2014).

2.4.2. Heating

Four main benefits received by treating crude oil emulsions via heating are reduction of viscosity, increase in droplets, paraffin crystals dissolution, and the increase in density difference between oil and water. Viscosity reduces as the crude oil is heated and this allows the water droplets to settle at a much faster rate. While this may vary from one crude oil to another, the chart below can be used as a general approximation of viscosity/temperature relationship of crude oil (courtesy of AMEC Paragon).

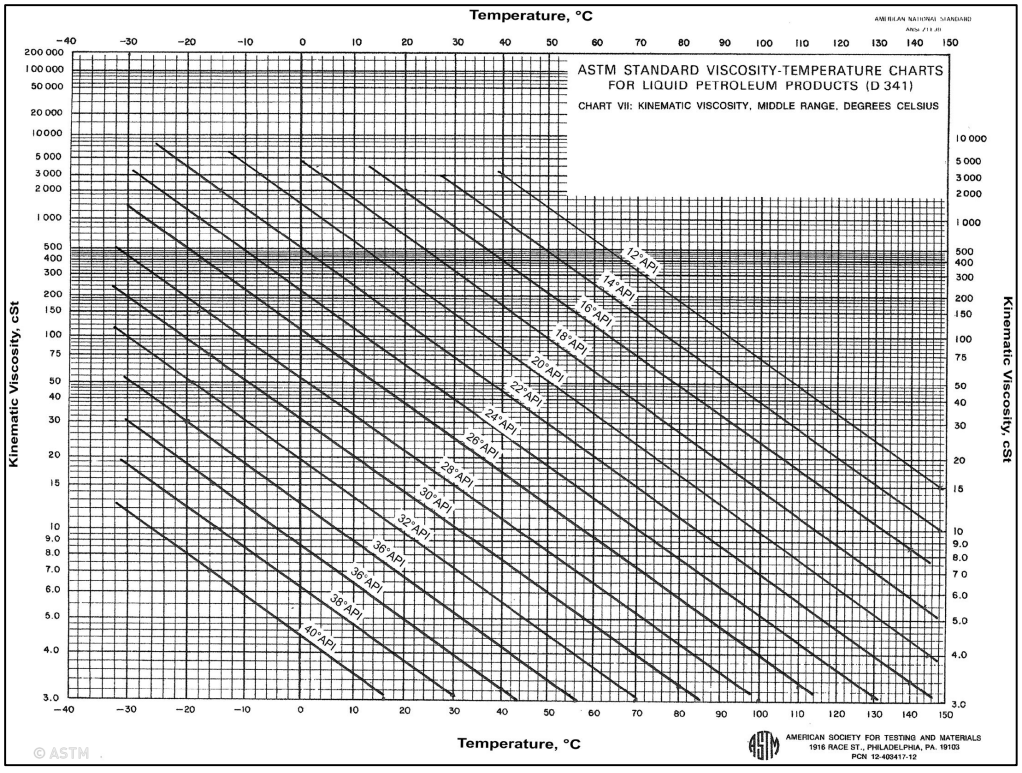

Figure 3 - Relationship of Viscosity and Temperature of Crude Oil (AMEC Paragon)

In addition to reducing viscosity, heat also increases the droplets' molecular movements. This will promote coalescence. There are reported cases where heat deactivates emulsifiers such as paraffin crystals and enhance the action of chemical demulsifiers, thus allowing them to work more efficiently.

Heat may increase the density difference between oil and water which allows settling to occur more quickly. This is especially good for light oils as it is normally transported at temperatures below 83°C.

2.5. Rag Layer

2.5.1. Definition

Rag layer is defined as the complex multiple emulsion of oil, water, solids, and surface active species and can be contributed by the slow coalescence mechanics which then results in the accumulation of material. (Madjlessikupai, et. al., 2012)

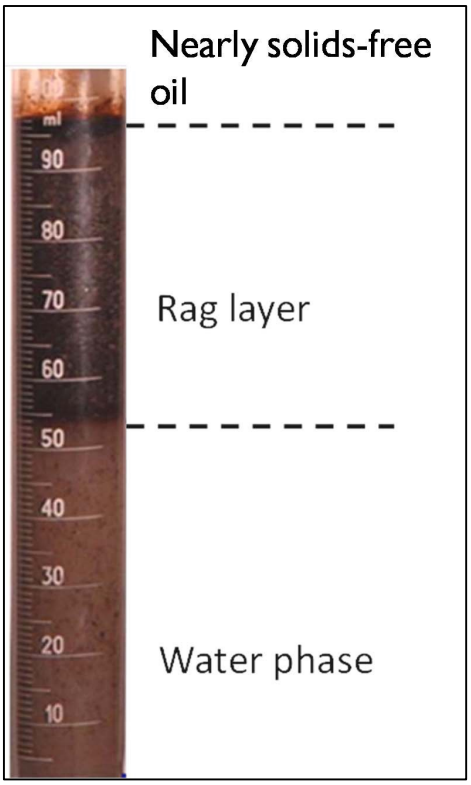

Figure 4 - Rag Layer in Water and Oil Mixture (Madjlessikupai, et. al., 2012)

Rag layers are asphaltenic, thus implying that it has the highest level of nitrogen functional groups, aromatics and carboxylics (Madjlessikupai, et. al., 2012). In addition to that, Manar (2012) also highlighted that the asphaltenic nature in rag layers also meant that that the rag layer precipitates in pentane, hexane, or heptane but soluble in toluene or benzene.

2.5.2. Rag Layer Formation

Varadaraj and Brons (2007) associated the formation of rag layer with the presence of surface-active crude oil polar, the asphaltenes and naphthenic acids, along with the small particulates or solids that were taken during crude oil extractions.

Based on a paper by Saadatmand and Yarranton (2008), rag layer can be formed due to two phenomenon: the first is when the coalescence rate of the water droplet is lower than its accumulation rate. The other is due to the accumulation of fine oil-wet solids being held together by interfacial tension forces.

However, it was also mentioned on the same paper that the reasoning behind the formation of rag layer build up has not yet been fully understood. Therefore, what may have worked on one particular scenario may not work on another. Such examples include the use of demulsifier or chemical additives.

2.5.3. Continuous Phase of Rag Layer

Madjlessikupai et. al (2012) had tested two methods to determine the continuous phase of rag layer emulsions. Samples of rag layers were placed in bottles of Milli-Q water and toluene to determine its diffusion characteristics. Both bottles were then shaken to allow the rag layer to diffuse. It was found that a clear solution was formed in the bottle containing rag layer and toluene while the rag layer in the bottle with Milli-Q appeared to be dispersed in water.

This can be seen in Figures 5 and 6 where the rag layer in the Milli-Q solution remained undiluted while the rag layer mixed with toluene were fully diluted.

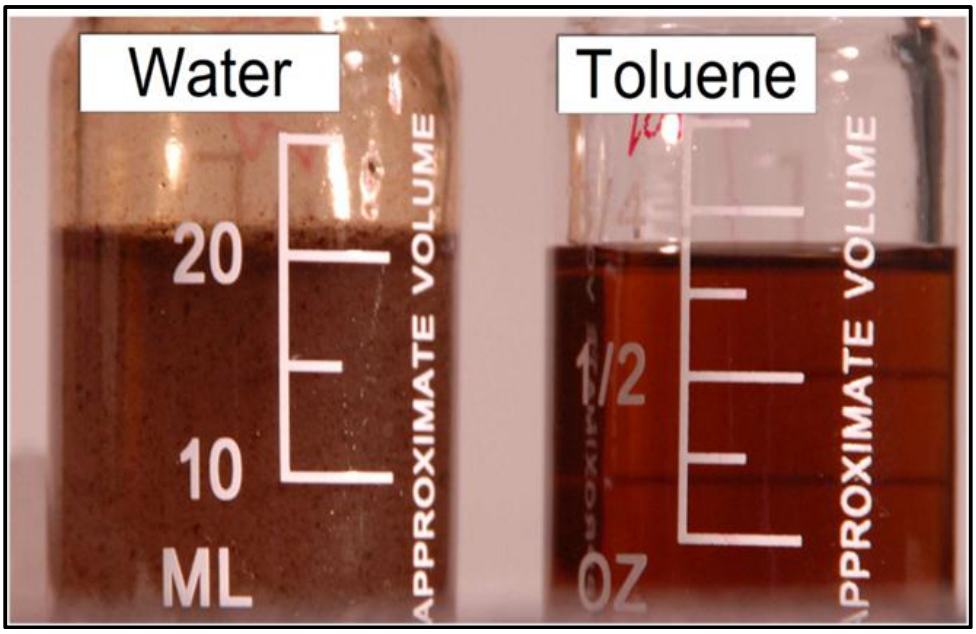

Figure 5 - Rag Layer in Toluene and Water (Madjlessikupai, et. al., 2012)

Figure 6 - Rag Layer Fully Diluted in Toluene (Madjlessikupai, et. al., 2012)

CHAPTER 3

METHODOLOGY

3.1. Rag Layer Production of 70% Crude Oil, 30% Water Mixture

To simulate the rag layer production in crude oil and water mixture, a mixture mirroring those found in the field needs to be created. This involved mixing 70% of each of the following with 30% artificially produced water:

- Crude Oil – Sample A and Sample B (well head samples).
- 30% synthetic macrocrystalline wax with 70% Isopar V.
- 30% synthetic microcrystalline wax with 70% Isopar V.

The micro and macro wax solutions were prepared by mixing a 30:70 wax to ExxonMobil Chemical's Isopar V ratio.

For a 50ml solution, 15g of wax is mixed with 35g Isopar V before being heated in a beaker at 70°C. The melted wax is then kept in an incubator at 80°C to ensure that it does not solidify.

3.2. Characterization of Rag Layer and Crude Oil

The characterizations of rag layer and crude oil will both take into account the environment in the field. This includes taking into consideration of the equipment present on the platform such as the separator.

The following tests will be conducted to characterize the rag layer and crude oil:

1. Rheology tests.
2. Cross polarized microscopy.
3. Pour point tests.
4. Differential scanning calorimetry.
5. Bottle tests.
6. Water content

The operating condition for the tests are:

- Working temperature range: 50°C to 15°C for all crude oil and 70°C to 15°C for wax.
- Shear rate for rheometer: 10^0 to 10^3.
- Cycles done for pour point tests: 6 cycles.

3.2.1. Rheology Tests – Rheometer

The rheology tests will be conducted on the Discovery Hybrid Rheometer by TA Instruments. The geometry used is a crosshatched geometry to reduce the slip effect while conducting the experiment.

In addition to that, the crosshatched geometry will also be able to accommodate the different gaps, based on the 10x of the maximum particle size rule of thumb. The size of the particles is determined via CPM.

Temperature sweep at three different shear rates of 10 1/s, 100 1/s and 400 1/s are performed. Temperature ranges for each sample is listed in Table 1 below.

Table 1 - Temperature Range for Rheometer Temperature Sweep

Sample	Temperature Range
Sample A	15°C to 60°C
Sample B	0° to 35°C
Macrocrystalline	10°C to 60°C
Microcrystalline	25°C to 85°C

3.2.2. Cross Polarized Microscopy

The cross-polarized microscopy (CPM) utilized a digital microscope by Olympus. The microscope is equipped with a cross-polarized filter that allows only a certain spectrum of light to pass through.

The wax appearance and disappearance temperature, as well as the wax particle size and type can be extracted from the image captured.

Different samples will be exposed to different temperature ranges and cooling to determine the wax appearance temperature (WAT) and wax disappearance temperature (WDT). Table 2 lists down the starting temperature for WAT and WDT determination for the different samples.

Table 2 - WAT and WDT Starting Temperature

Sample	WAT Starting Temp.	WDT Starting Temp.
Sample A	60°C	10°C
Sample B	35°C	0°C
Macrocrystalline	45°C	25°C
Microcrystallline	80°C	45°C

3.2.3. Pour Point Tests

The pour point tests are conducted to determine the pour point temperature of the wax, which is the temperature at which the wax completely gels up. This is performed using a pour point tester by PSL Systemtechnik.

The tests are conducted for 6 cycles and at different temperatures, depending on the sample tested. The maximum temperatures set for each sample are as per Table 3.

Table 3 - Maximum Temperature for PPT

Sample	Maximum Temperature
Sample A	55°C
Sample B	40°C
Macrocrystalline	70°C
Microcrystalline	70°C

3.2.4. Bottle Tests

Bottle tests are conducted to observe the condition of the crude when mixed with formation water over time. Some may form emulsion while others may separate almost immediately.

The sample is prepared inside a 250ml beaker and stirred using a high-speed stirrer. Once a predetermined temperature is reached, the sample is mixed with 30% production water and stirred for 15 minutes before being separated into four different 45ml centrifuge bottles.

The temperatures and stirring rates for each sample are as per Table 4 while the composition of the production bottle is as Table 5.

Table 4 - Bottle Test Temperature and Stirring Rates

Material	Temperature	Stirring Rates
Sample A	65°C	10000RPM
Sample B	65°C	9000RPM
Macrocrystalline	75°C	9000RPM
Microcrystalline	75°C	9000RPM

Table 5 - Composition of Production Water

Components	Amount (g/L)
$HaHCO_3$	5.126
KCl	0.2646
NaCl	6.0114
$BaCl = 2H_2O$	0.0067
$SrCl_2 = 6H_2O$	0.0141
$MgCl = 6H_2O$	0.075
$CaCl = 2H_2O$	0.2344

Different temperature and stirring rates were set for different samples. From studies conducted in the same flow assurance lab, it was found that the best temperature and stirring rate to produce the highest amount of rag layer are 65°C and 10,000 RPM.

However, in the case of both macro and micro crystalline wax, the temperature is set 10°C higher than the optimal conditions as the melting temperature of both wax is within the 60°C region. Therefore, a temperature of 75°C is set to ensure that the wax is properly dissolved.

All but Sample A was stirred at 9,000 RPM as spillage is detected at 10,000 RPM for these samples.

CHAPTER 4

RESULTS AND DISCUSSION

Experiments were conducted on the two crude samples, Sample A and B, as well as on the Sasolwax micro and macrocrystalline wax mixtures. Rheological behaviour, wax appearance and disappearance temperature, pour point, freezing point temperatures and bottle tests are assessed.

4.1. Pour Point and Freezing Point

The pour point and freezing point temperatures of the actual and synthetic crude oils were taken using the pour point tester available. The following results were captured:

i. Sasolwax macrocrystalline wax – Run 01, directly after pouring

Table 6 – Macrocrystalline Wax PPT – Run 01

Cycles	**1**	**2**	**3**	**4**	**5**	**6**
FP	34.5	34.2	34.4	34.3	34.3	34.4
PP	36	36	36	36	36	36
Mean (FP)	34.35					
SD (FP)	0.104880885					

ii. Sasolwax macrocrystalline wax – Run 02, directly after sample 01

Table 7 - Macrocrystalline Wax PPT - Run 02

Cycles	**1**	**2**	**3**	**4**	**5**	**6**
FP	34.1	34.2	34.2	34.3	34.0	34.3
PP	36	36	36	36	36	36
Mean (FP)	34.18					
SD (FP)	0.116904519					

iii. Sasolwax macrocrystalline wax – Run 03, 24 hours after run 02

Table 8 - Macrocrystalline Wax PPT - Run 03

Cycles	1	2	3	4	5	6
FP	34.4	34.3	34.3	34.2	34.2	34.8
PP	36	36	36	36	36	36
Mean (FP)	34.37					
SD (FP)	0.2251					

iv. Sasolwax microcrystalline wax – Run 01, directly after pouring

Table 9 - Microcrystalline Wax PPT - Run 01

Cycles	1	2	3	4	5	6
FP	36.8	36.7	36.7	36.8	36.7	36.7
PP	39	39	39	39	39	39
Mean (FP)	36.73					
SD (FP)	0.0516					

v. Sasolwax microcrystalline wax – Run 02, 24 hours after run 01

Table 10 - Microcrystalline Wax PPT - Run 02

Cycles	1	2	3	4	5	6
FP	37.0	36.5	36.6	36.8	36.7	36.5
PP	39	39	39	39	39	39
Mean (FP)	36.68					
SD (FP)	0.1940					

vi. Sample B crude – Run 01, directly after pouring

Table 11 - Sample B PPT - Run 01

Cycles	1	2	3	4	5	6
FP	6.6	7.8	8.2	8.7	8.7	8.9
PP	9	9	9	9	9	9
Mean (FP)	8.15					
SD (FP)	0.8596					

vii. Sample B crude – Run 02, 24 hours after run 01

Table 12 - Sample B PPT - Run 02

Cycles	1	2	3	4	5	6
FP	9.6	9.6	9.8	10.0	9.9	10.2
PP	12	12	12	12	12	12
Mean (FP)	9.85					
SD (FP)	0.2345					

viii. Sample A crude – Run 01, directly after pouring

Table 13 - Sample A PPT - Run 01

Cycles	1	2	3	4	5	6
FP	26.3	26.2	26.2	26.0	26.0	26.0
PP	27	27	27	27	27	27
Mean (FP)	26.12					
SD (FP)	0.1213					

ix. Sample A crude – Run 02, directly after run 01

Table 14 - Sample A PPT - Run 02

Cycles	1	2	3	4	5	6
FP	25.7	25.8	26.0	26.0	26.1	25.9
PP	27	27	27	27	27	27
Mean (FP)	25.91					
SD (FP)	0.1343					

x. Sample A crude– Run 03, 24 hours after run 02

Table 15 - Sample A PPT - Run 03

Cycles	1	2	3	4	5	6
FP	26.3	26.6	26.7	26.8	26.8	27.1
PP	27	27	27	27	27	30
Mean (FP)	26.72					
SD (FP)	0.2409					

Based on the data from the pour point tester, it was observed that both macrocrystalline and microcrystalline wax have similar pour point and freezing point temperatures throughout their cycles. The standard deviation from the cycles was also low, further confirming the results received.

Pour point is defined as the lowest temperature at which a sample of the fluid exhibits flow characteristics under defined condition while freezing point is the Temperature at which a substance turns from liquid to solid state (PSL Systemtechnik, 1999). In complex solution, the freezing point is always moved to lower temperature (freezing point depression).

In the case of the Sample B crude oil, there were differences in both the pour point temperature and the freezing point temperature between the test conducted directly after pouring, and the one done after 24 hours wait. It was suspected that the some of the lighter ends may have evaporated and thus causing the differences in temperature. This was also proved based on the pour point tests

conducted by a post-graduate student whereby it was observed that as time passes, the pour point temperature of Sample B increases.

4.2. Wax Appearance and Disappearance Temperature - CPM

The wax appearance temperature is considered to be the temperature that the first wax crystal started to form. There are many ways of determining the wax appearance temperature and these include the use of cross-polarized microscope, density and viscosity variation, differential scanning calorimetry and many others (Neto, et al., 2009)

The results below refers to those found from the use of cross-polarized microscopy:

i. Sample A crude

Table 16 - WAT of Sample A

Run No.	**1**	**2**	**3**
WAT	41.0	35.0	37.7
Mean	37.9		
SD	2.4536		

Table 17 - WDT of Sample A

Run No.	**1**	**2**	**3**
WDT	49.3	44.5	45.5
Mean	46.4		
SD	2.0677		

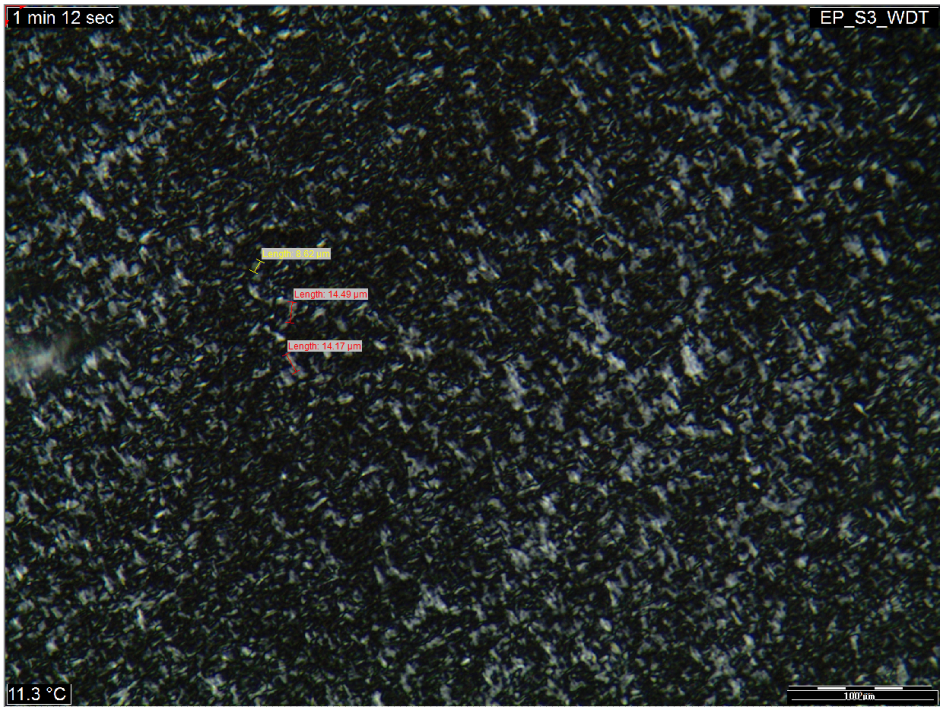

Figure 7 - Wax Particles for Sample A at 11.3°C

Based on Figures 7 and 8, it was observed that the wax present in Sample A crude consist of both macro and micro wax. Based on an average of three sample size taken, it was found that the largest wax particles for Sample A is 12.43 microns, as seen in Figure 7.

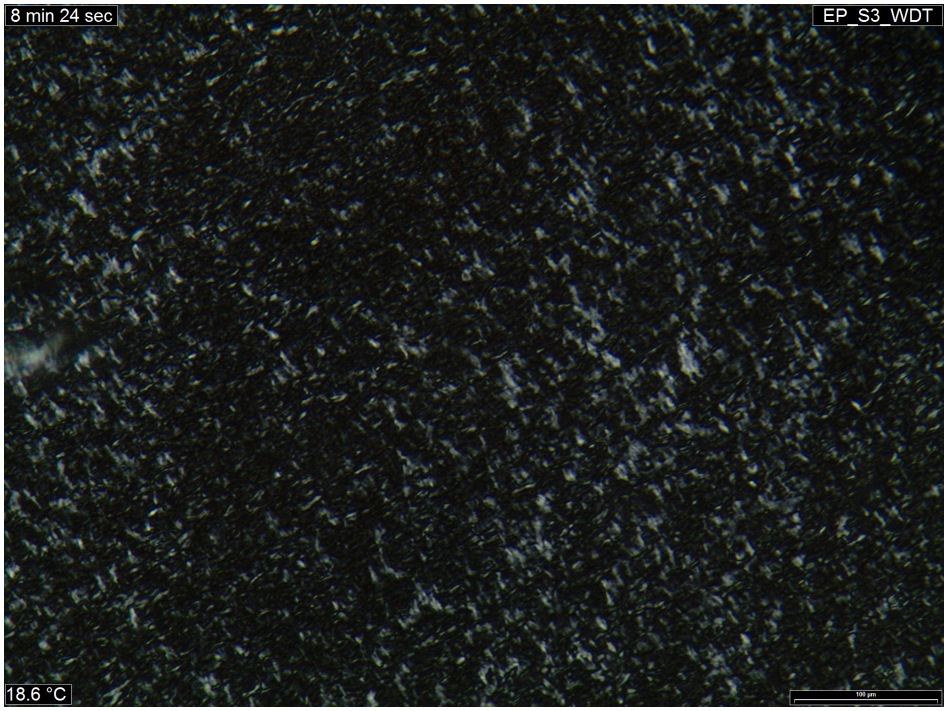

Figure 8 - Wax at 18.6°C on Sample A

ii. Sample B crude

Table 18 - WAT of Sample B

Run No.	1	2	3
WAT	22.8	22.3	24.8
Mean	23.3		
SD	1.0801		

Table 19 - WDT of Sample B

Run No.	1	2	3
WDT	24.1	25.2	25.5
Mean	24.9		
SD	0.6018		

Based on the results from Tables 18 and 19, it was observed that the WAT and WDT are 23.3°C and 24.9°C respectively. However, it was observed that if the same sample is utilized for subsequent testing, the WAT and WDT tend to increase. This may be due to the evaporation of the light ends in Sample B, similar to that observed in the pour point measurement.

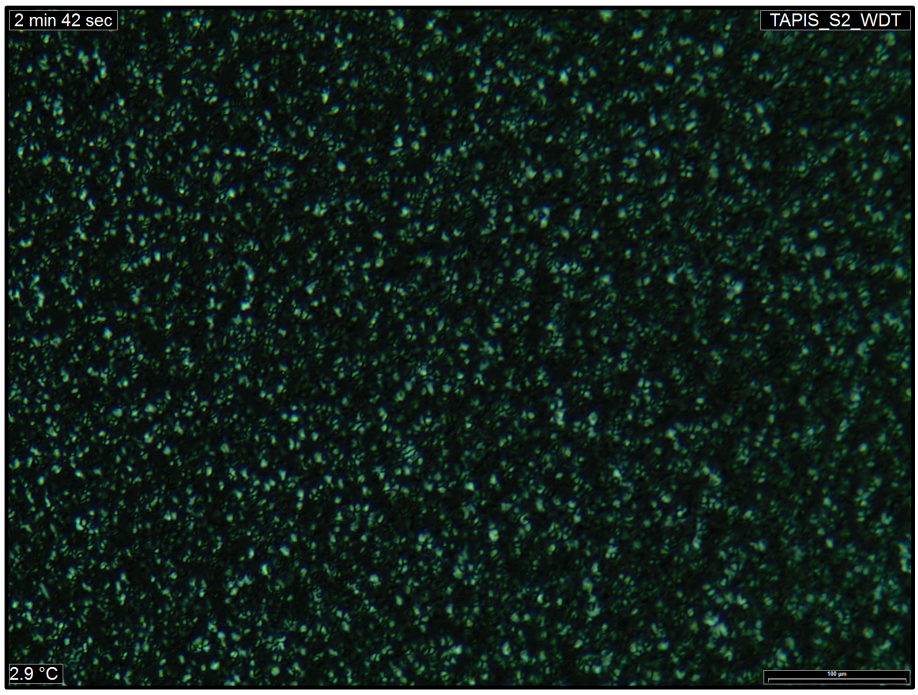

Figure 9 - Wax at 2.9°C on Sample B

Micro wax was prevalent on Sample B crude. Based on the measurements in Figure 10, the average size of the largest particle in Sample B was found to be 11.58 microns.

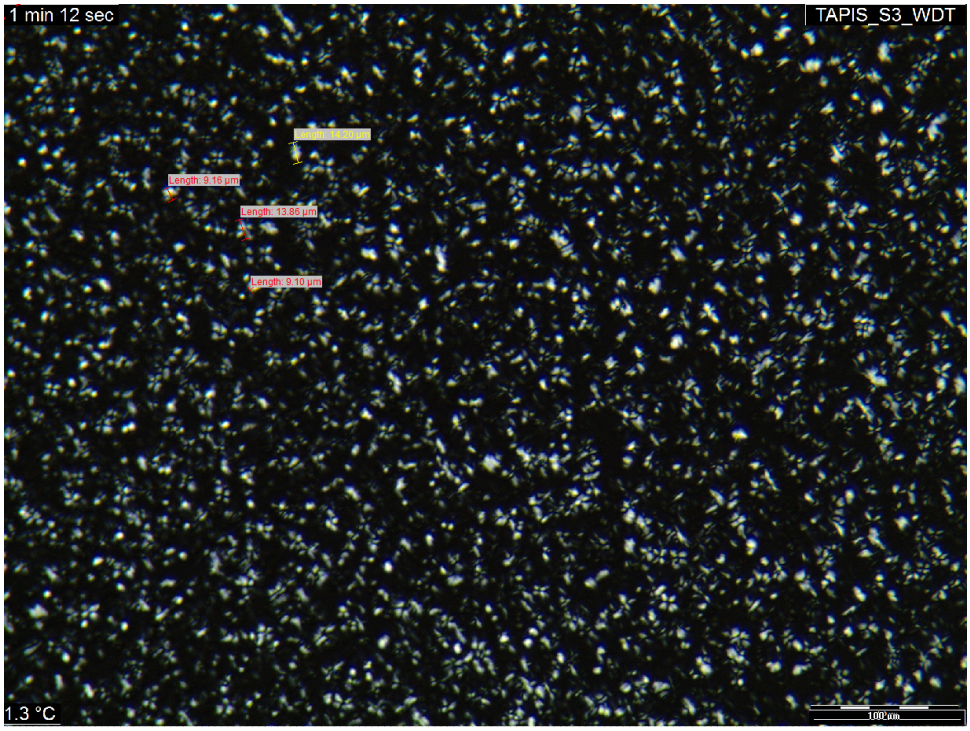

Figure 10 - Wax Particles for Sample B at 1.3°C

iii. Sasolwax Macrocrystalline Wax

Table 20 - WAT of Macrocrystalline Wax

Run No.	**1**	**2**	**3**
WAT	37	37.3	37.5
Mean	37.3		
SD	0.2517		

Table 21 - WDT of Macrocrystalline Wax

Run No.	**1**	**2**	**3**
WDT	38.4	38.2	39.4
Mean	38.7		
SD	0.6429		

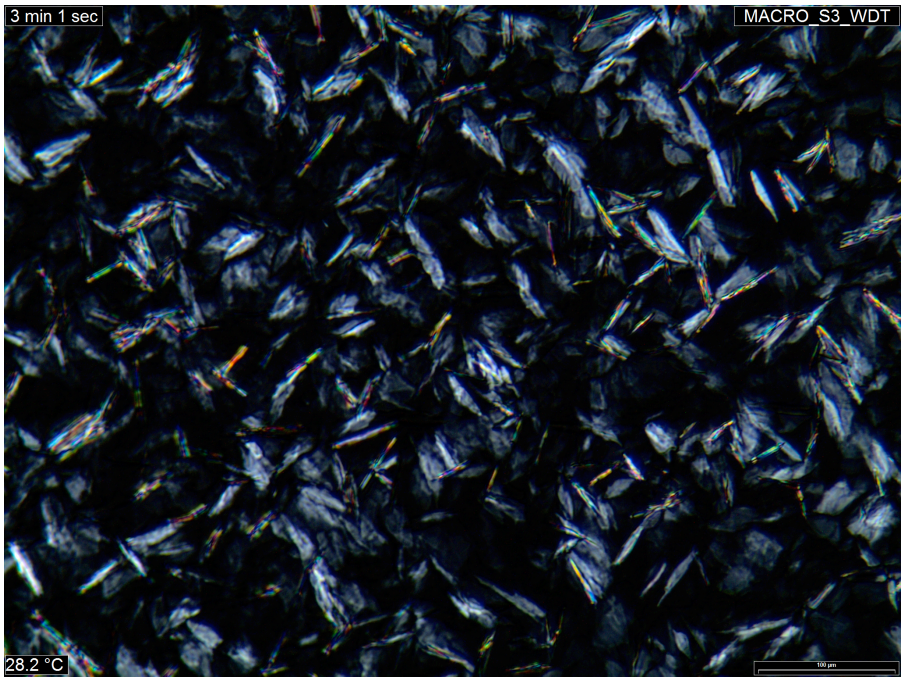

Figure 11 - Wax at 27.1°C on Macrocrystalline Wax Solution

As expected, the wax found on the Sasolwax Macrocrystalline solution consists purely of macro wax as seen in Figure 11.

Based on Figure 12, the average size of the largest wax particles is 67.73 microns. As recorded in Table 20 and 21, the WAT and WDT of the macrocrystalline wax is 37.3°C and 38.7°C respectively.

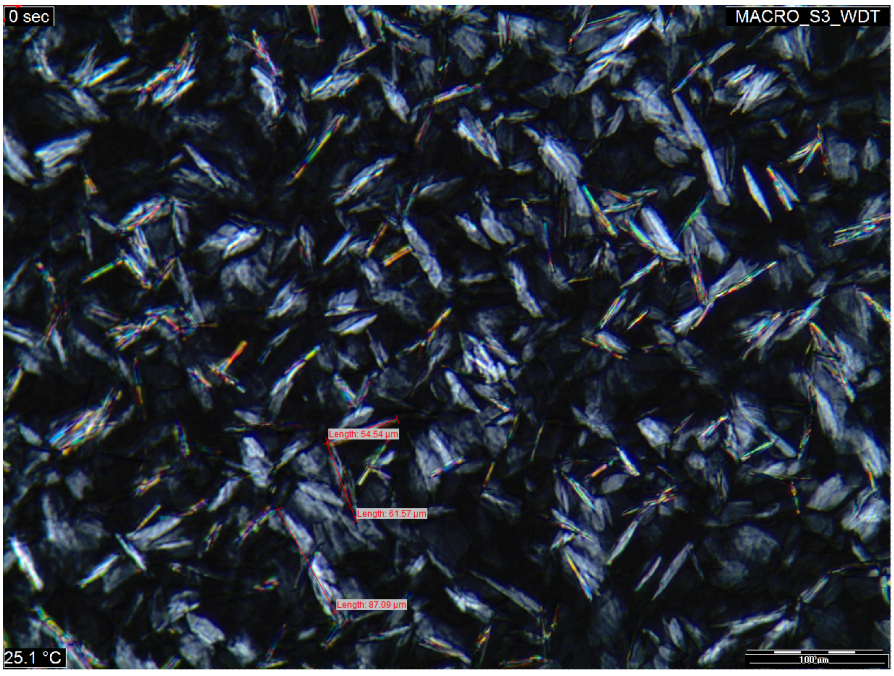

Figure 12 - Wax Particles for Macrocrystalline Wax at 25.1°C

iv. Sasolwax Microcrystalline Wax

Table 22 - WAT of Microcrystalline Wax

Run No.	1	2	3
WAT	64.6	66.6	66.3
Mean	65.8		
SD	0.8806		

Table 23 - WDT of Microcrystalline Wax

Run No.	1	2	3
WDT	72.2	71.8	71.8
Mean	71.9		
SD	0.1886		

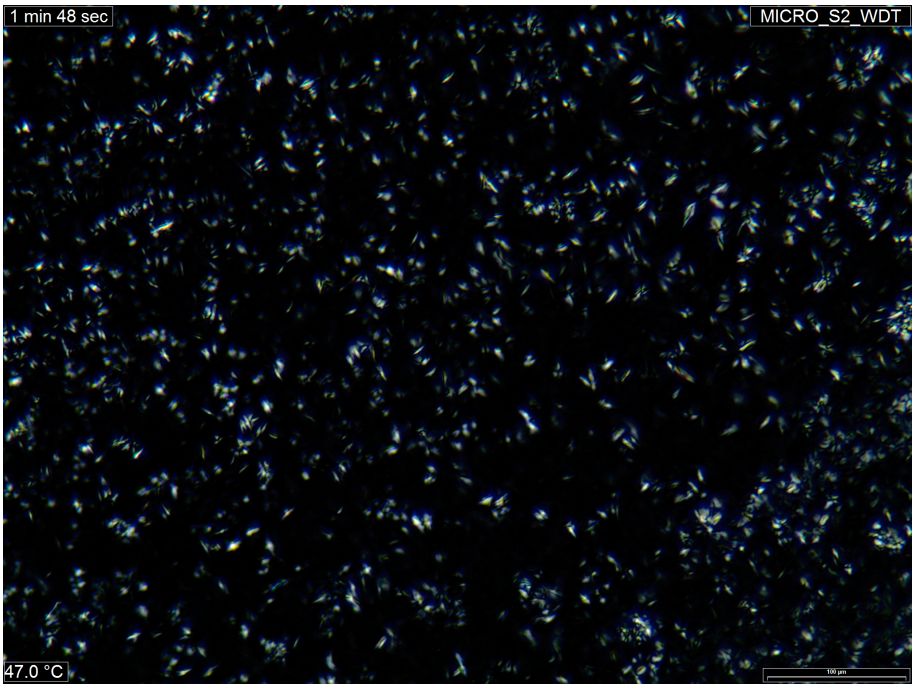

Figure 13 - Wax at 36.8°C on Microcrystalline Wax Solution

Figure 13 showed that only microcrystalline wax is present in the solution. In addition to that, Table 22 and 23 recorded a WAT and WDT of 65.8°C and 71.9°C respectively for the microcrystalline wax solution.

Based on Figure 14, it is observed that the average size of the largest crystals to be 14.89 microns.

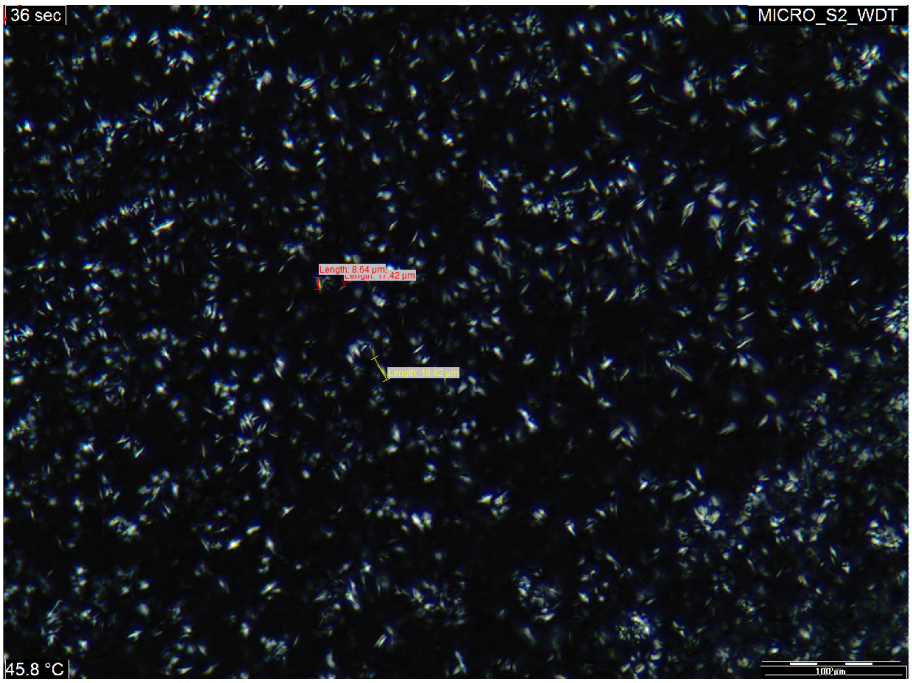

Figure 14 - Wax Particles for Microcrystalline Wax at 15.8°C

The table below summarises the mean of the wax appearance and disappearance temperatures, and the average size of the largest crystals of the crude oils and synthetic waxes.

Table 24 - Summary of WAT and WDT

	Sample A	Sample B	Macro Wax	Micro Wax
WAT (°C)	37.9	24.4	37.3	65.8
WDT (°C)	46.4	26.6	38.7	71.9
PPT (°C)	27.0	10.5	36.0	39.0
FPT (°C)	26.3	9.0	34.2	36.7
Crystal Size (microns)	12.43	11.58	67.73	14.89

4.3. Rheometer – AR-G2 TA Instruments

The AR-G2 rheometer from TA Instruments was used to measure the rheological characteristics of crude oils and the waxes. A temperature sweep was done at a pre-determined temperature and at three different shear rates. These are 10 s^{-1}, 100 s^{-1} and 400 s^{-1}.

Assuming that a 12-inch flowline is used subsea, the shear rates are equivalent to 15,000 bbl/day for 10 s^{-1}, 150,000 bbl/day for 100 s^{-1} and 600,000 bbl/day for 400 s^{-1}.

i. Synthetic Macrocrystalline Wax

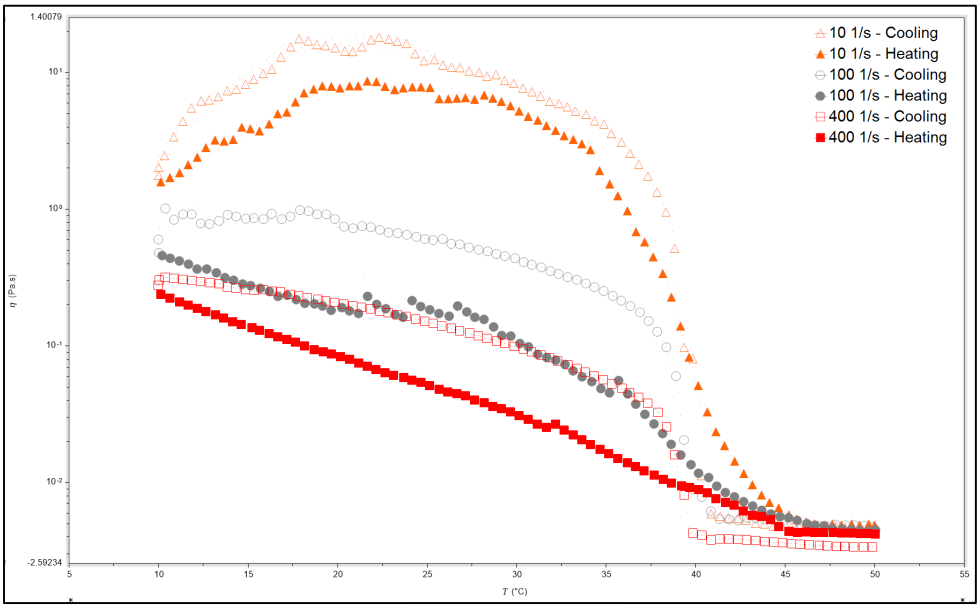

Figure 15 - Temperature Sweep Result - Macro Wax

The temperature sweep on the synthetic macrocrystalline wax was done between a temperature of 60°C to 10°C at three different shear rates, which were 10 s^{-1}, 100 s^{-1}, and 400 s^{-1}. The highest viscosity was observed at 10 s^{-1} cooling sweep between 20°C to 25°C. A drop in viscosity was observed at 10 1/s when the sample should already be in gel condition at the lower temperatures. It is possible that wall slippage had occurred at the lower temperature of the 10 1/s shear rate.

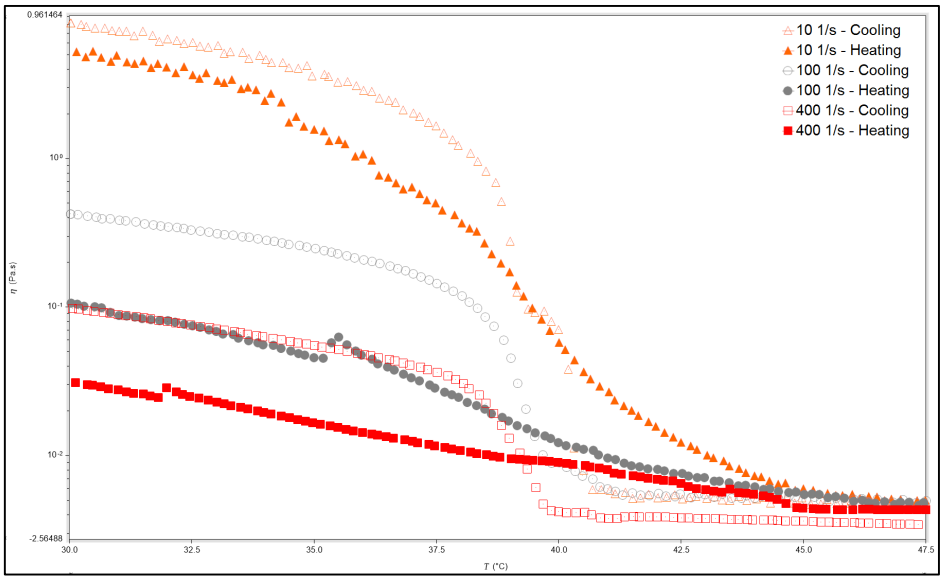

Figure 16 - Large Increase in Viscosity between 39°C to 40°C

Moreover, a large increase in viscosity was seen between the temperatures of 39°C to 40°C, as observed in Figure 16. This observation is further strengthen by observing the cooling result in Figure 17, where an increase was observed at 41°C for 10 1/s, and 39°C for both the 100 1/s and 400 1/s shear rates.

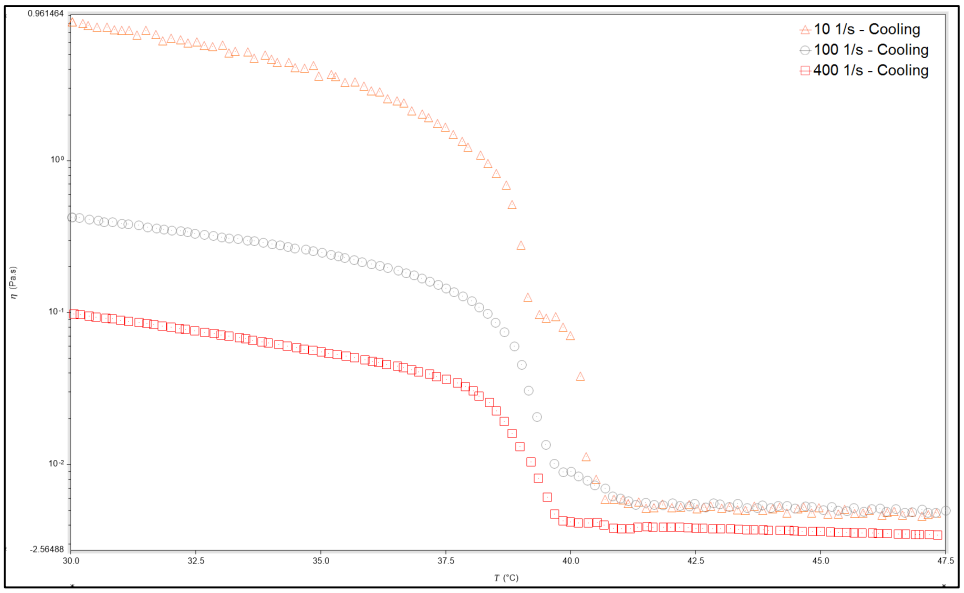

Figure 17 - Cooling Result for Macro Wax

This also correlates well with the results found from CPM, as the WAT was found to be at 38.6°C.

ii. Synthetic Microcrystalline Wax

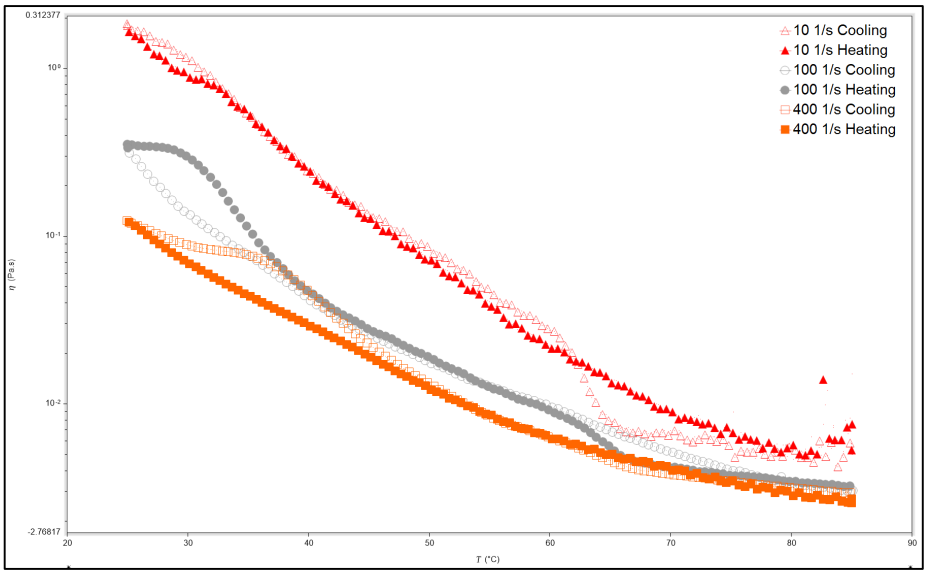

Figure 18 – Temperature Sweep Result – Micro Wax

The same temperature sweep was conducted on the synthetic micro wax between the temperature of 25°C to 85°C. The shear rates applied are 10 s^{-1}, 100 s^{-1}, and 400 s^{-1} to reflect different production rates.

As observed in Figure 19, viscosity is the highest at 10 s^{-1}. In addition to that, viscosity appears to increase as temperature decreases due to the accumulation of wax at the lower temperature.

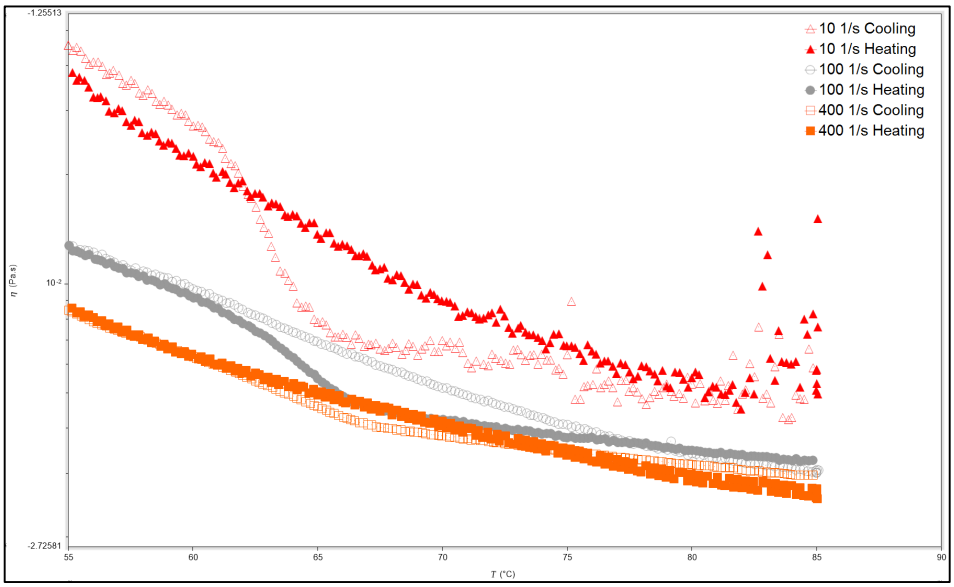

Figure 19 – Large Increase in Viscosity at 65.0°C

The large increase in viscosity as observed in Figure 20 at 65.0°C suggested the wax appearance temperature for the microcrystalline wax. Unlike the rest of the samples, viscosity of the micro wax started to increase 65°C and not at other temperatures, even at different shear rates.

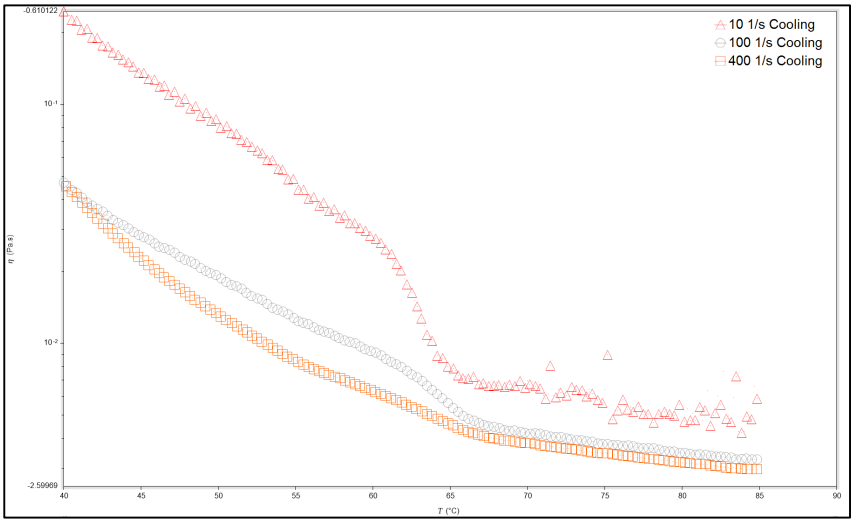

Figure 20 - Cooling Result for Micro Wax

In comparison with the results from the cross-polarized microscopy for the microcrystalline wax, a small difference of only 0.8°C was observed. Therefore, it can be concluded that the wax appearance temperature of the microcrystalline wax to be around 65°C.

iii. Sample A

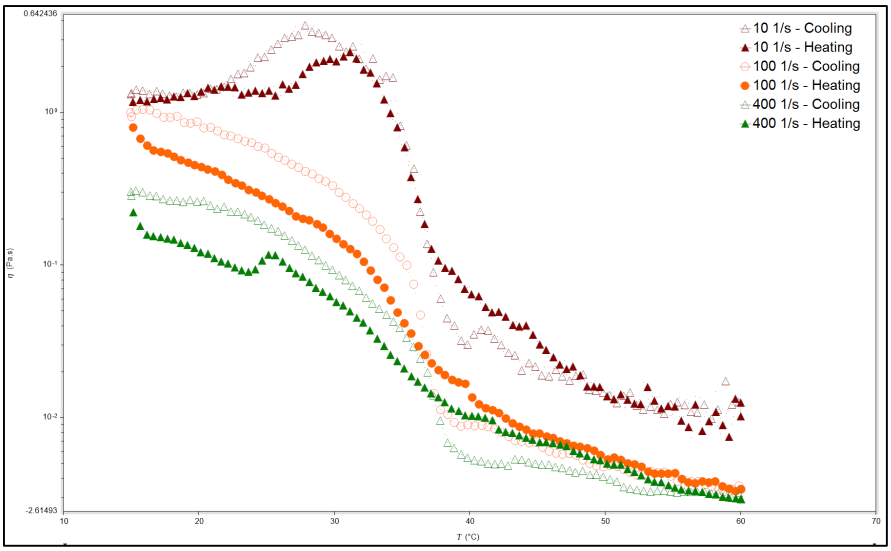

Figure 21 - Temperature Sweep Result - Sample A

The temperature ramping for Sample A was set between the range of 60°C and 15°C at a shear rate of 10 s^{-1}, 100 s^{-1} and 400 s^{-1}. As observed in Figure 21, viscosity was highest at a shear rate of 10 s^{-1}. A large drop in viscosity was also observed in Figure 21, which may be attributed to wall slippage.

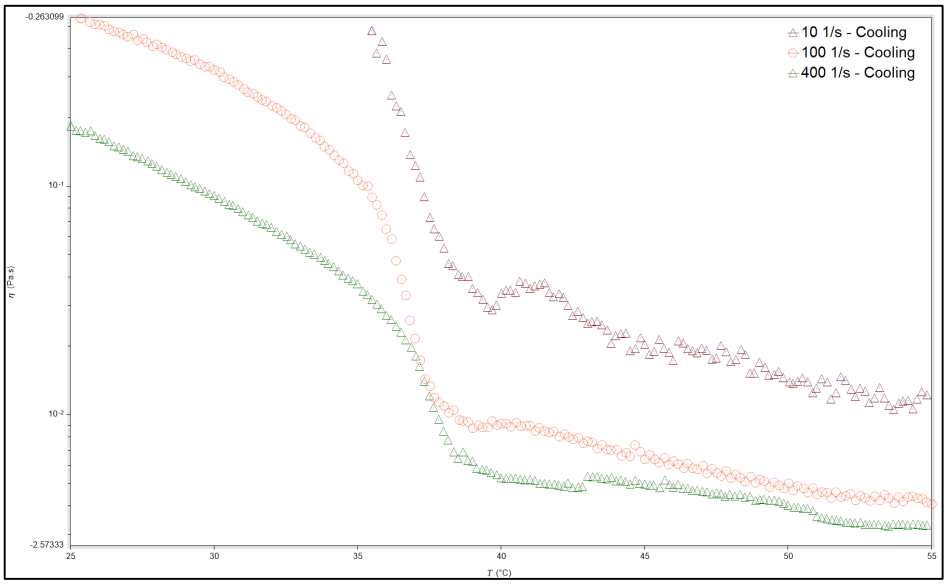

Figure 22 - Large Increase in Viscosity between 37.5°C to 40°C

Figure 22 suggests a wax appearance temperature of 37.5°C to 40°C for Sample A. At 10 1/s, it was observed that the large increase in viscosity was found at 40°C while both the 100 1/s and 400 1/s recorded a large increase in viscosity at 37.5°C. This also corresponds well with the wax appearance temperature recorded from the CPM which is at 37.9°C.

iv. Sample B

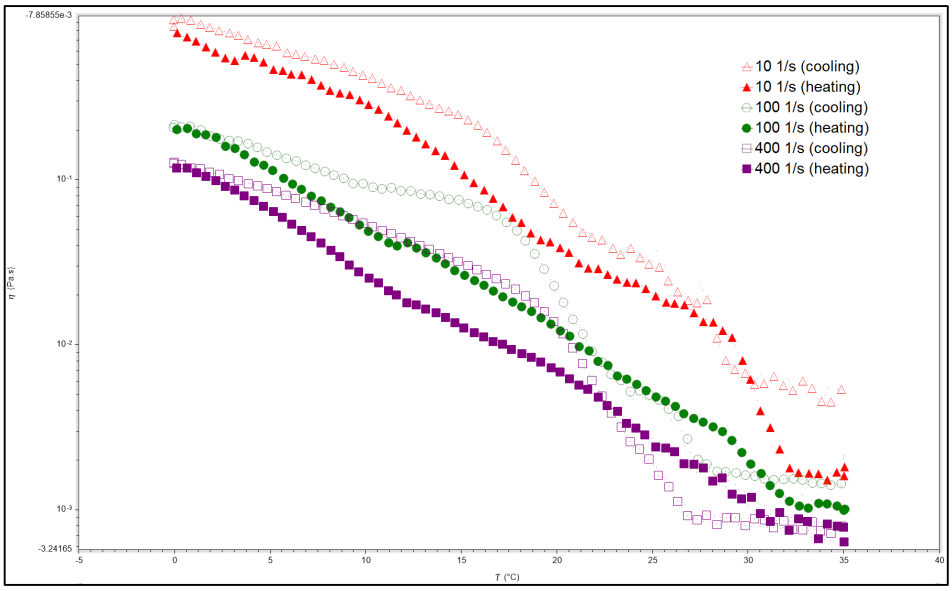

Figure 23 - Temperature Sweep Result - Sample B

Sample B ran at temperatures between 35°C and 0°C, at a shear rate of 10 s^{-1}, 100 s^{-1} and 400 s^{-1}. As the temperature decreases, the viscosity of Sample B increases, with the highest viscosity observed during the cooling period for the shear rate of 10 s^{-1}.

Figure 24 below shows the cooling result for Sample B. Shear thinning was observed as viscosity reduces with higher shear rate.

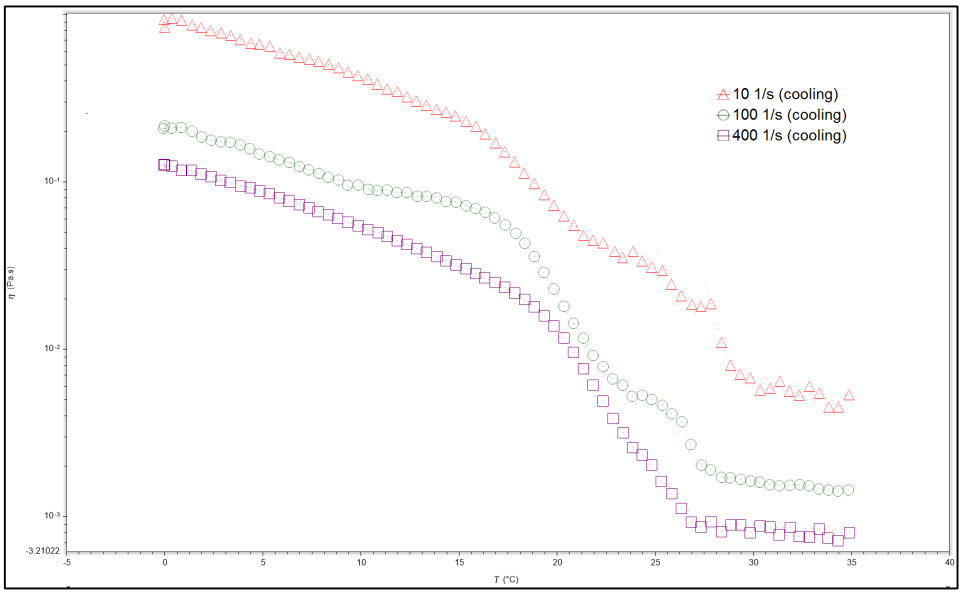

Figure 24 – Cooling Result for Sample B

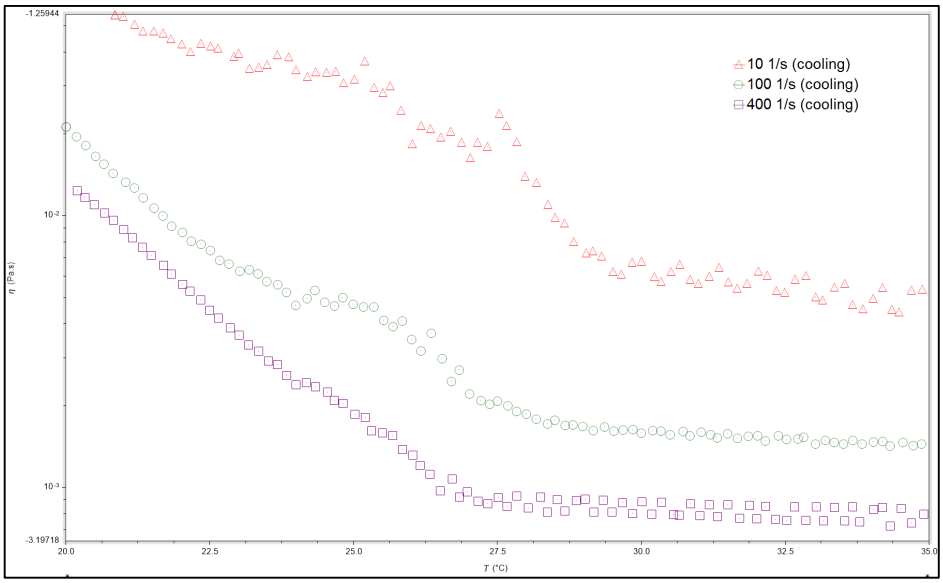

Figure 25 - Large Increase in Viscosity between 22°C to 30°C

The wax appearance temperature is different for all three shear rates as the increase at 10 1/s started at 27.5°C, while both the 100 1/s and 400 1/s experienced large increase in viscosity at a lower temperature of 26°C.

In general, all samples experienced shear thinning, whereby the viscosity reduced when the shear rate was increased. Wall slippage was a possibility for both Sample A and the synthetic macrocrystalline wax, due to the large drop in viscosity at the lower temperatures where the sample should have already been in gel condition. It was difficult to determine the wax disappearance temperature of the samples as the viscosity reduced gradually.

4.4. Differential Scanning Calorimetry - microDSC

A small sample (50mg) is taken from each of the four samples to test the wax appearance temperature of each material. The samples are placed in the microDSC7 evo microcalorimeter to observe the thermodynamic activities during the wax precipitation.

i. Sample A

The sample was cooled from a temperature of 85°C to -30°C and the reading is taken every 0.5s. Figure 26 below shows the DSC result for Sample A. The onset temperature for Sample A is at 35.1°C, thus suggesting the wax appearance temperature for the sample.

When compared with the results from the CPM and rheometer, a difference of 2°C was observed. This may be due to the sensitivity of the microcalorimeter.

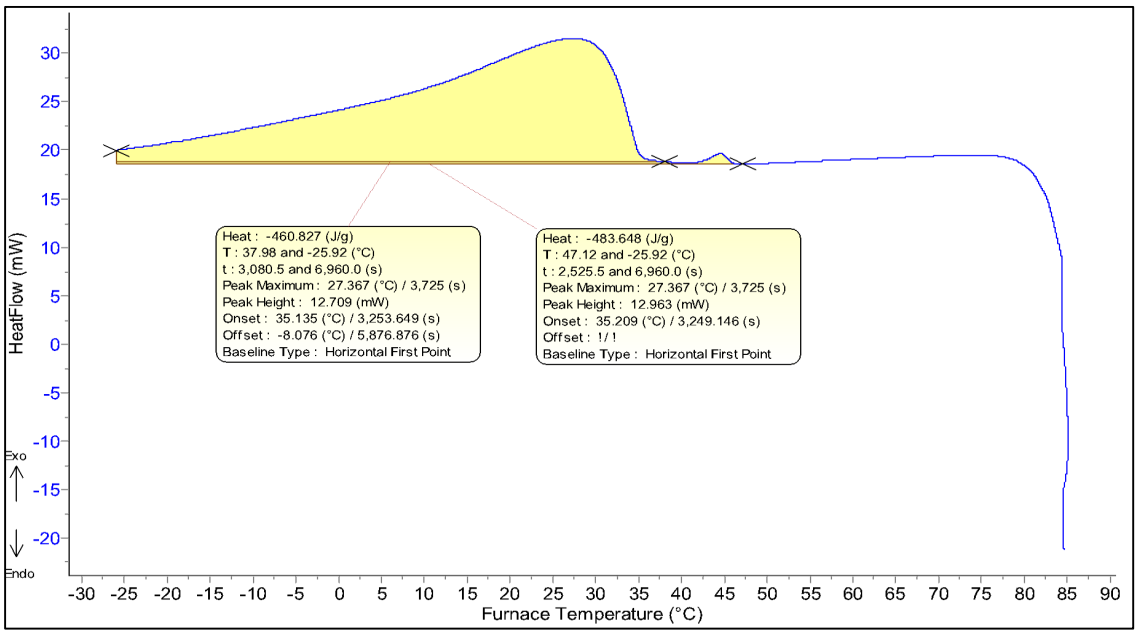

Figure 26 - DSC Result for Sample A

ii. Sample B

As observed in Figure 27, Sample B was cooled in the microcalorimeter from 25°C to -25°C. The onset temperature captured was at 19.9°C, resulting a 3°C difference when compared with the rheometer and a 5°C difference when compared with the CPM.

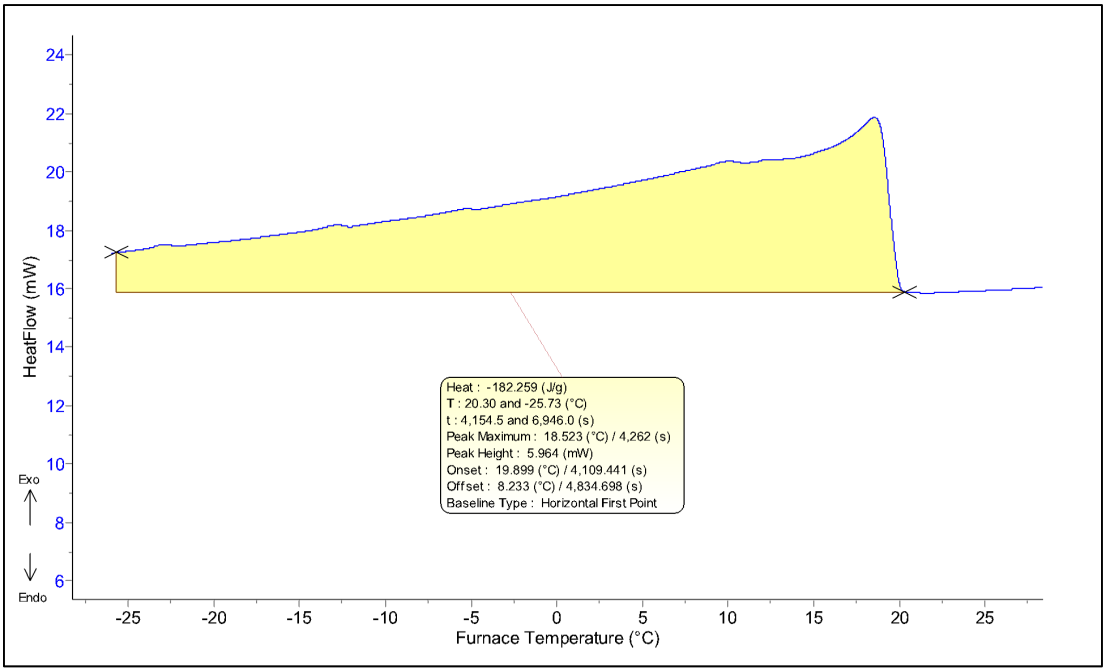

Figure 27 - DSC Result for Sample B

iii. Synthetic Macrocrystalline Wax

Figure 28 shows the DSC result for the synthetic macrocrystalline wax. An onset temperature of 37.6°C is observed for the macro wax, which suggests the wax appearance temperature for the sample.

In comparison with the rheometer, the result is almost similar as the rheometer recorded an increase in viscosity between 39°C and 40°C, whereas the CPM recorded the first wax appearing at 38.6°C. Therefore, the wax appearance temperature for the synthetic macrocrystalline wax is conclusive, between the ranges of 37°C to 40°C.

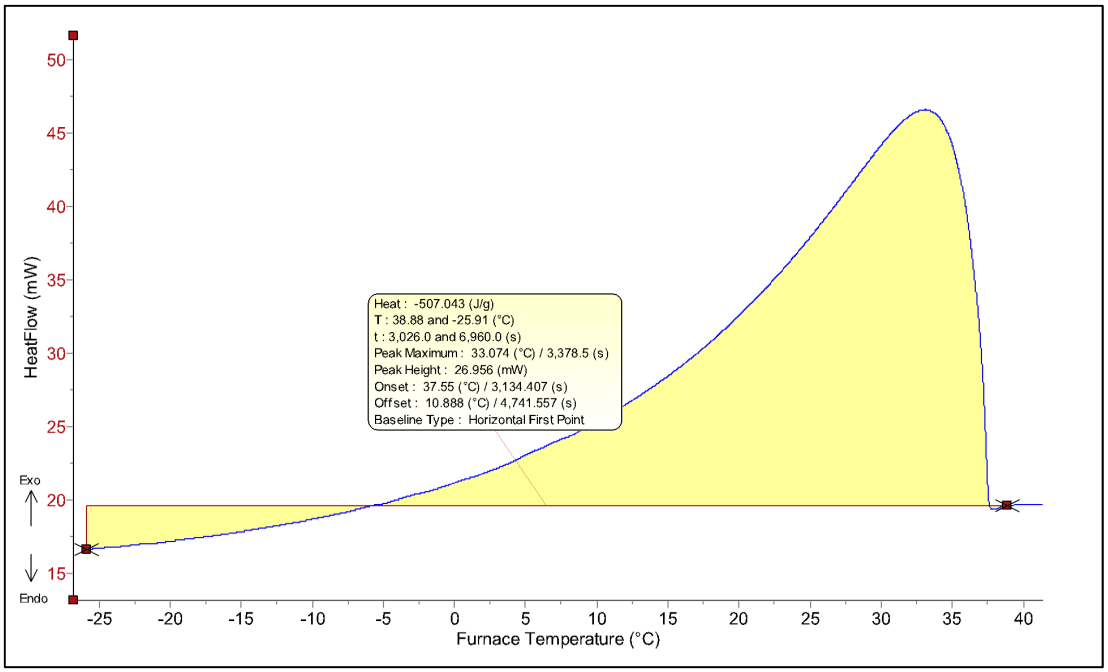

Figure 28 - DSC Result for Synthetic Macrocrystalline Wax

iv. Synthetic Microcrystalline Wax

In Figure 29, the first onset temperature for the synthetic microcrystalline wax is recorded at 65.9°C. Therefore, this is the temperature suggested as the wax appearance temperature of the wax.

This result is similar to both CPM and rheometer as both recorded a wax appearance temperature of 65.8°C and 65°C respectively. The small difference in the results suggest that the wax appearance temperature for the microcrystalline wax to be 65°C.

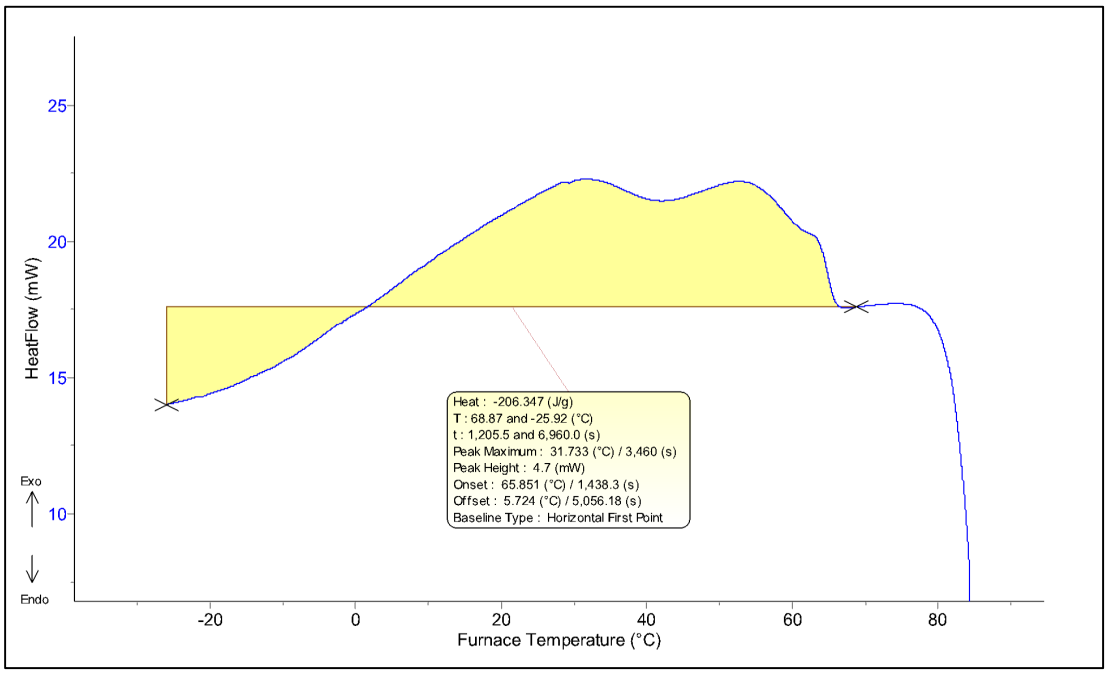

Figure 29 - DSC Result for Synthetic Microcrystalline Wax

Table 25 below is the collection of WAT recorded from all experiments.

Table 25 - WAT from All Measurements

Sample	CPM WAT	Rheometer WAT	DSC WAT	Average WAT
A	37.9°C	37.0°C	35.1°C	36.7°C
B	24.4°C	22.5°C	19.9°C	22.3°C
Macro Wax	37.3°C	39.0°C	38.6°C	38.3°C
Micro Wax	65.8°C	65.0°C	65.9°C	65.6°C

v. Sample A Rag Layer

Figure 30 below shows the DSC result for Sample A rag layer. A small heat was released at an onset temperature of 44.0°C. This suggests the wax appearance temperature for the rag layer of Sample A.

When compared with the DSC result found in Sample A, the onset temperature differs by 7°C, with the rag layer sample having the higher onset temperature. However, it should be noted that rag layer sample has been left for long time before being used. Therefore, there is a probability that the sample has been contaminated or that the lighter ends have evaporated.

A large peak was then observed at -11.9°C. This is suspected to be an increase due to the artificially produced water as this is also seen in other rag layer results.

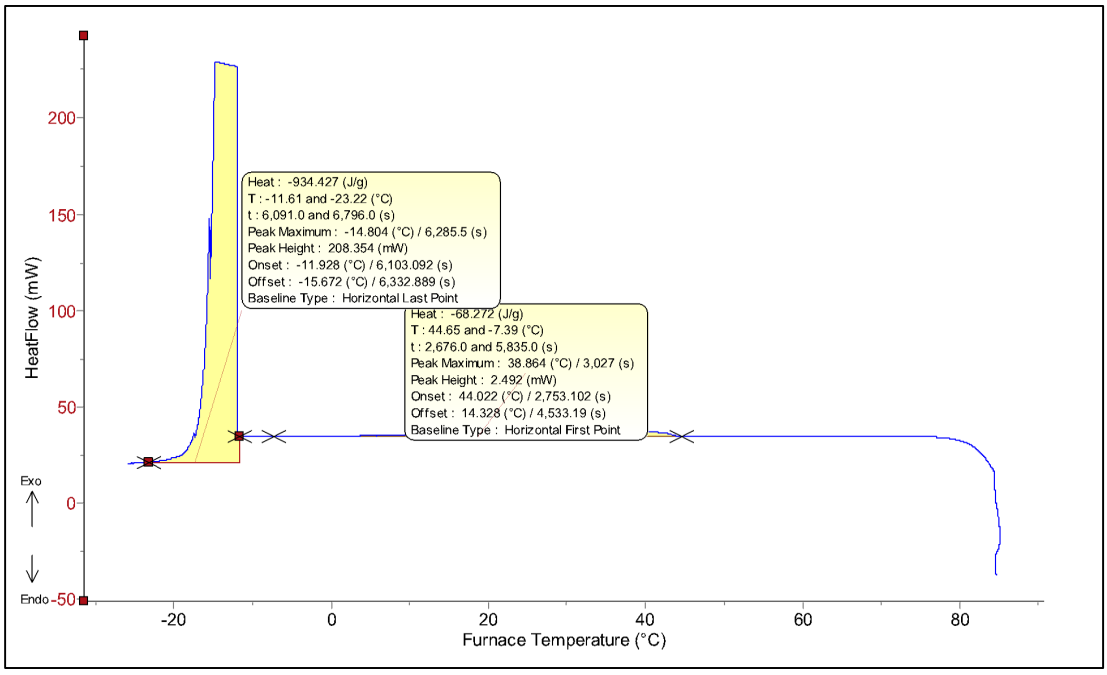

Figure 30 - DSC Result for Sample A Rag Layer

vi. Sample B Rag Layer

The rag layer for Sample B has a wax onset temperature of 32.7°C, as observed in Figure 31. This suggests the wax appearance temperature of the rag layer. As compared with the DSC result for Sample B crude oil, there was a large difference as the wax onset temperature for crude oil is 19.9°C as compared with the rag layer, which is at 32.7°C. Like the Sample A rag layer, this sample was also kept for a while before being used. Therefore, the lighter ends of the crude may have evaporated, causing an increase in the wax appearance temperature.

Much like the Sample A rag layer result, there was also a large heat released at -12.3°C. The artificially produced water is the suspect for the large heat release.

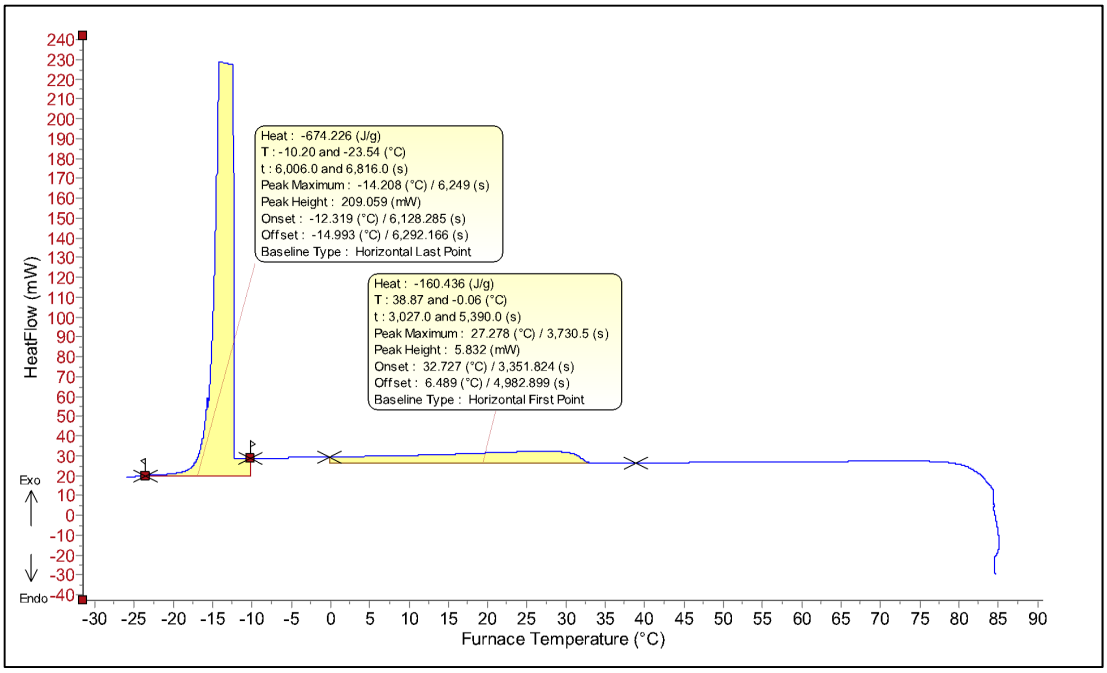

Figure 31 - DSC Result for Sample B Rag Layer

vii. Synthetic Microcrystalline Wax Rag Layer

The DSC result for the micro wax rag layer suggests a wax onset temperature of 74.6° as compared with 65.8°C originally obtained from the pure wax solution.

Figure 32 also shows a large heat release at -6.9°C, which is consistent with other rag layer results.

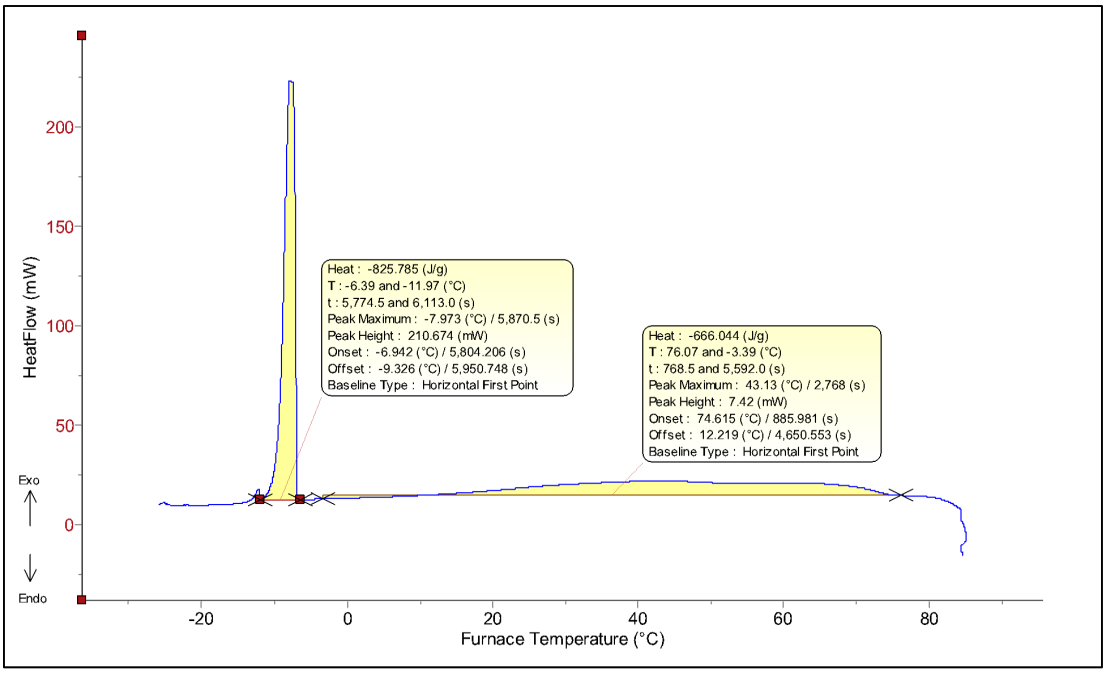

Figure 32 - DSC Result for Micro Wax Rag Layer

Based on the results received from the DSC, it was observed that all rag layer samples had an increase in the wax onset temperature as compared with the pure wax or crude sample, thus suggesting an increase in its WAT. Moreover, the large release of heat below 0°C is consistent with the artificially produced water present in the rag layer.

4.5. Bottle Tests

Bottle test is conducted on all of the samples to monitor the gravitational settling process of the samples. Each sample is mixed and heated to a pre-set speed and temperature to best simulate the conditions in the field.

The bottle test is conducted by mixing 70% of the sample or wax solution with 30% production water.

viii. Sample A (Mixed at 10,000RPM, 70°C, monitored at 70°C)

Sample A mixture produced a partially stable emulsion as a large amount of the mixture separated almost immediately when removed from the mixer. An oil in water emulsion is observed in the mixture, as shown in Figure 34.

When transferred from the beaker to the centrifuge bottles, the first two bottles consisted mainly of crude oil, whereas the third and fourth bottle had emulsion present in it.

Figure 33 highlights the bottle test result for Sample A. The mixture initially contained a large amount of emulsion and oil. However, by day one, the mixture is almost fully separated. The decrease in the oil content is attributed to evaporation when placed inside the incubator.

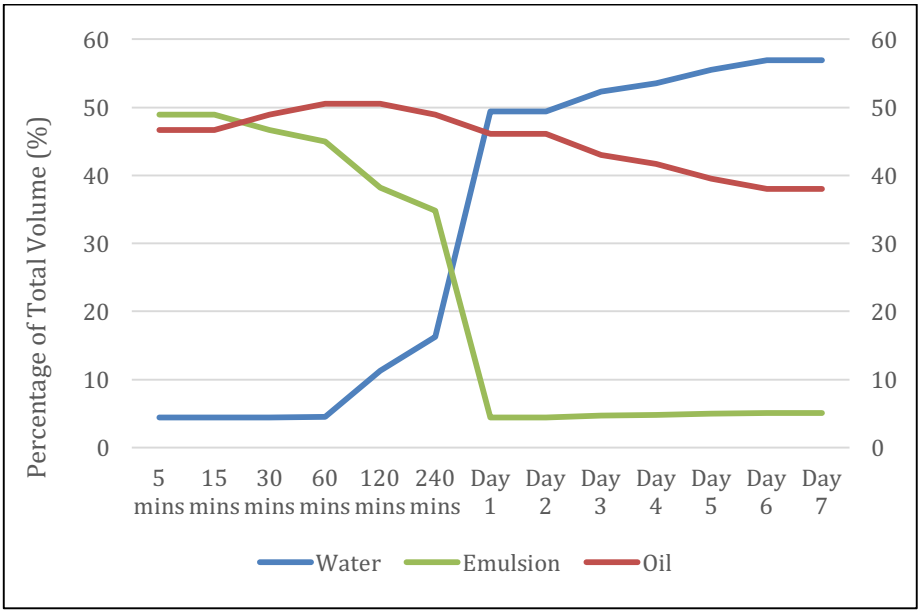

Figure 33 - Bottle Test Results for Sample A

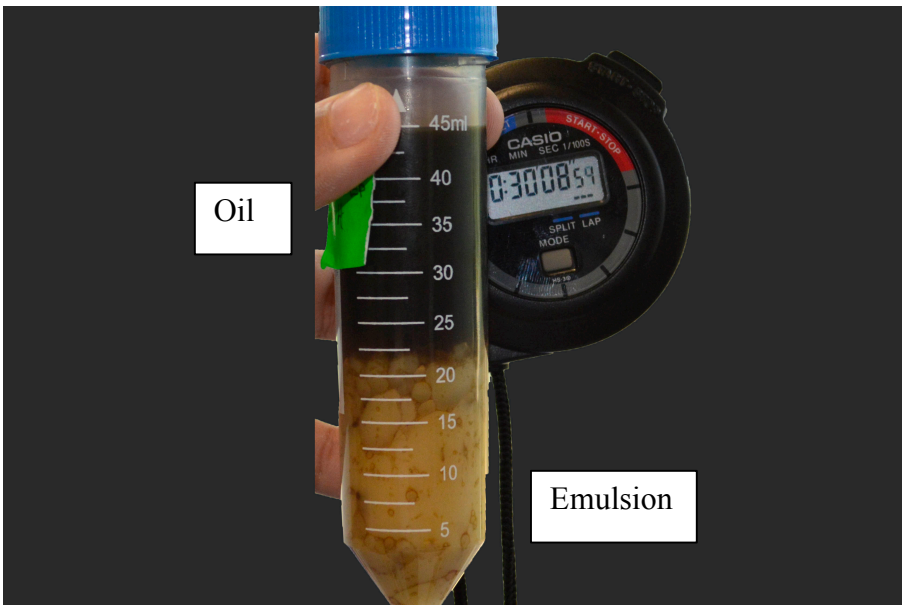

Figure 34 - Sample A Oil-in-Water Mixture at 30 Minutes from Bottle #3

The emulsion remained the same throughout the bottle test, with no visible clear separation of water.

There were also no clear presence of rag layer from the bottles with emulsion (bottle #3 and #4) but there are small amount of rag layer seen in bottle #1 and #2.

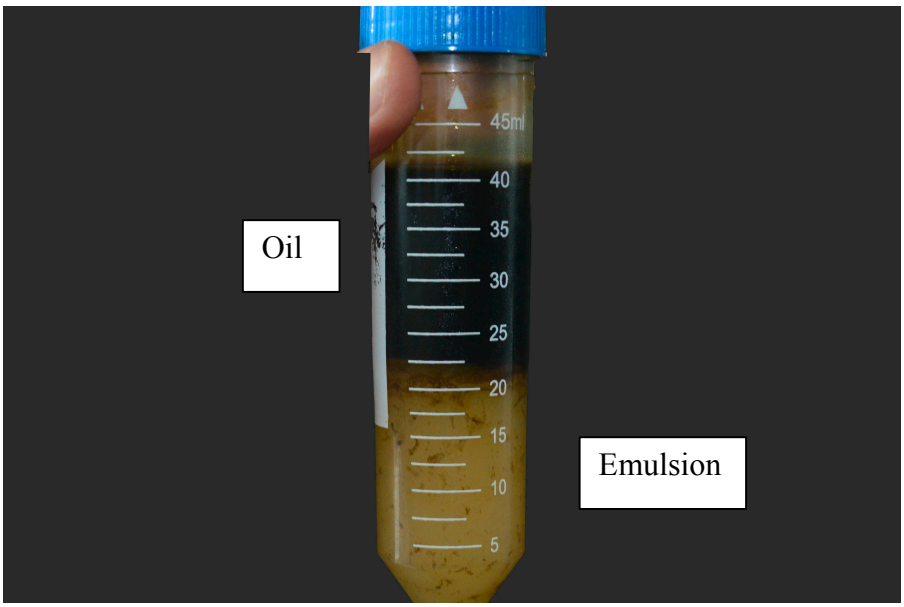

Figure 35 - Sample A Oil-in-Water Mixture, 1 Day, from bottle #3

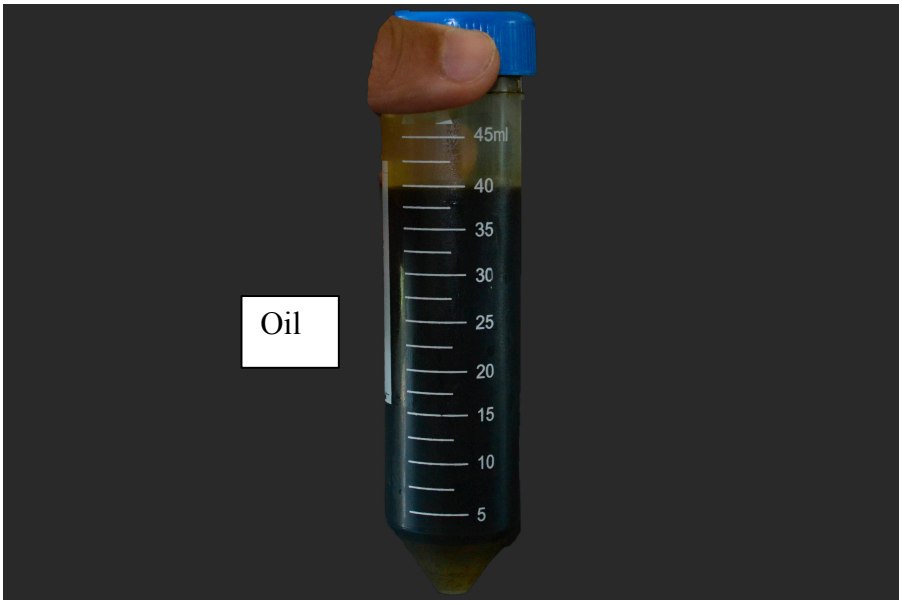

Figure 36 - Sample A Full Separation, 1 Day, from bottle #2

ix. Sample B (Mixed at 9,000RPM, 65°C)

Sample B produced three different layers of liquid which were crude oil, emulsion, and separated water. However, the amount of water recovered was only a small amount (7.5ml) as compared to the emulsion (22.5ml) and crude oil (12.5ml).

A tight emulsion was observed from Sample B. It took a significant amount of time for the crude to separate. Even after four hours of the bottle test, the mixture remained homogenous. Only after a day that the separation was visible though it has not been fully separated. This was also seen in Figure 37 below.

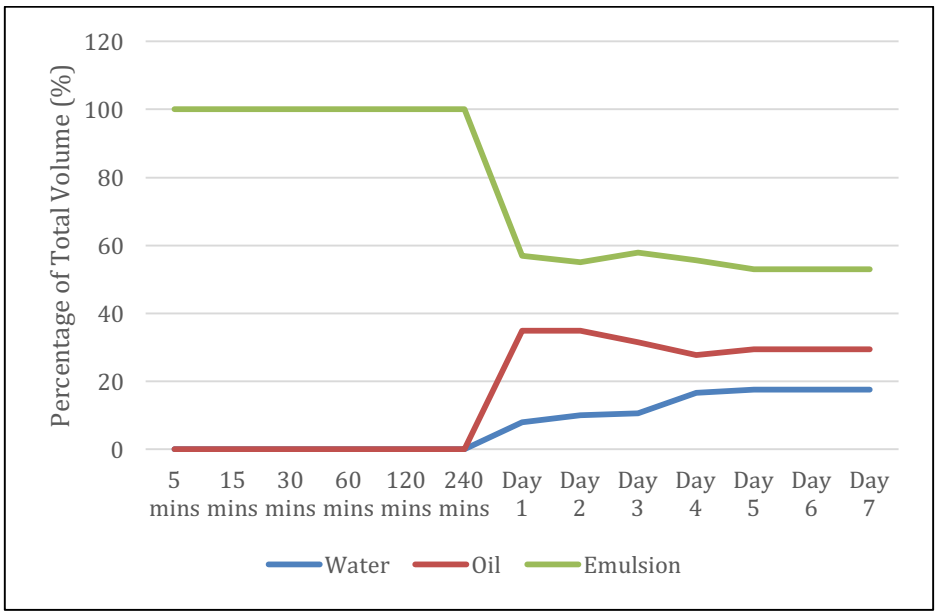

Figure 37 - Bottle Test Results for Sample B

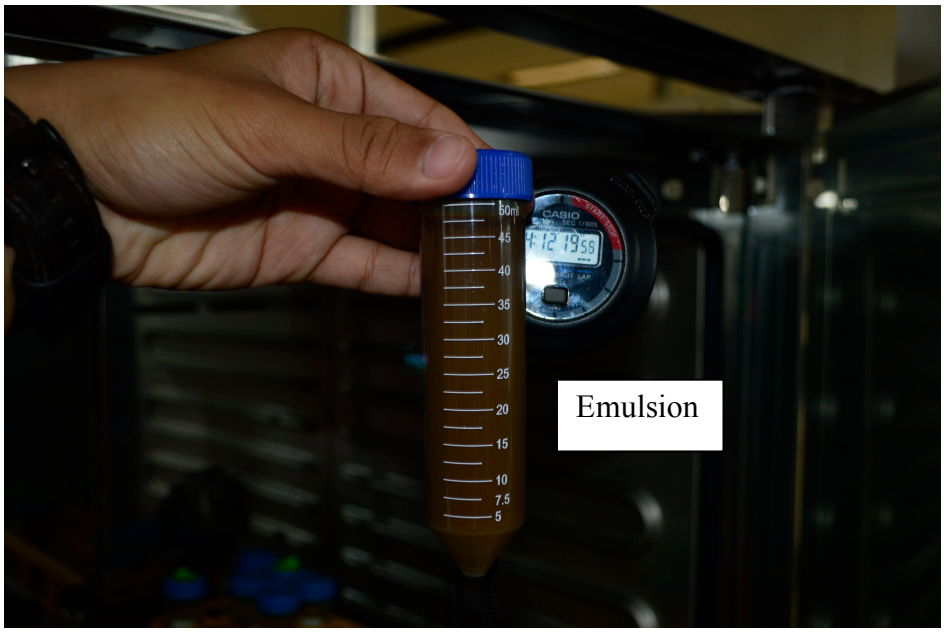

Figure 38 - Homogenous Solution after 4 Hours - Bottle #3

It can be concluded that Sample B will have a problem in the separator as it takes more time to separate than the standard separation time (30 minutes) inside the separator as observed in Figure 38 and 39.

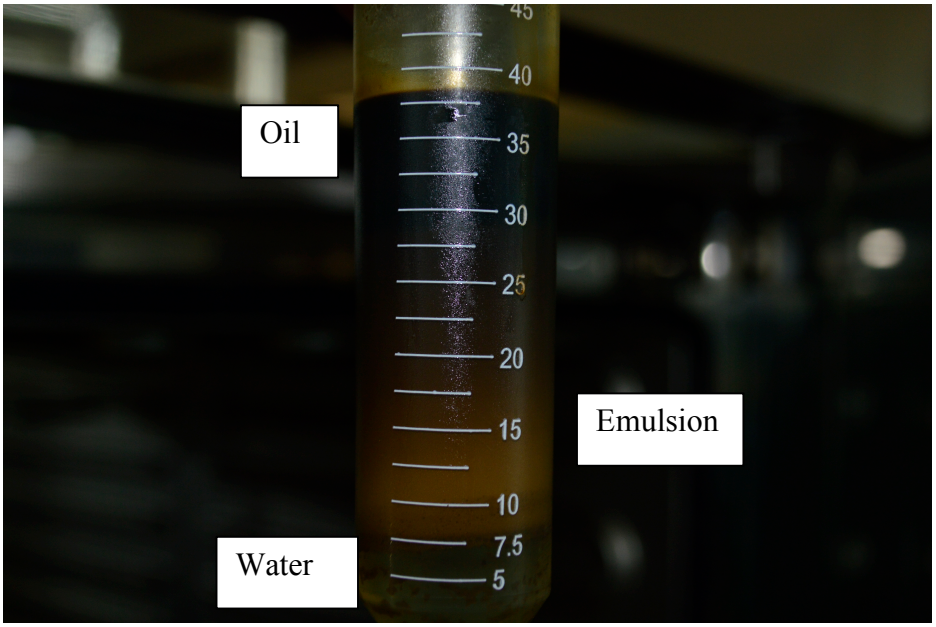

Figure 39 - Separated Mixture after 7 Days - Bottle #3

x. Synthetic Macrocrystalline Wax (Mixed at 9,000RPM, 75°C)

The sample of synthetic macrocrystalline wax separated almost immediately when removed from the mixer. Therefore, the separation could not be observed from the centrifuge bottles.

A mixture of 175 ml was made in a beaker and the first two bottles that was poured to from the beaker contained almost 100% of macrocrystalline wax. The third bottle contained 30 ml of wax and 15ml of water and the fourth bottle had only 5 ml of wax and 32.5 ml of water. This was done under the space of only 5 minutes.

Hence, it was concluded that the sample would not cause any problems in the separator as it separated quickly. Most of the sample can be recovered within 5 minutes, much less than the 30 minutes requirement for most separators.

In addition to that, it was also observed that the macrocrystalline wax mixture did not produce any rag layer, as seen in Figure 40. This was unlike the microcrystalline wax, where a white layer was observed between the water and wax layer.

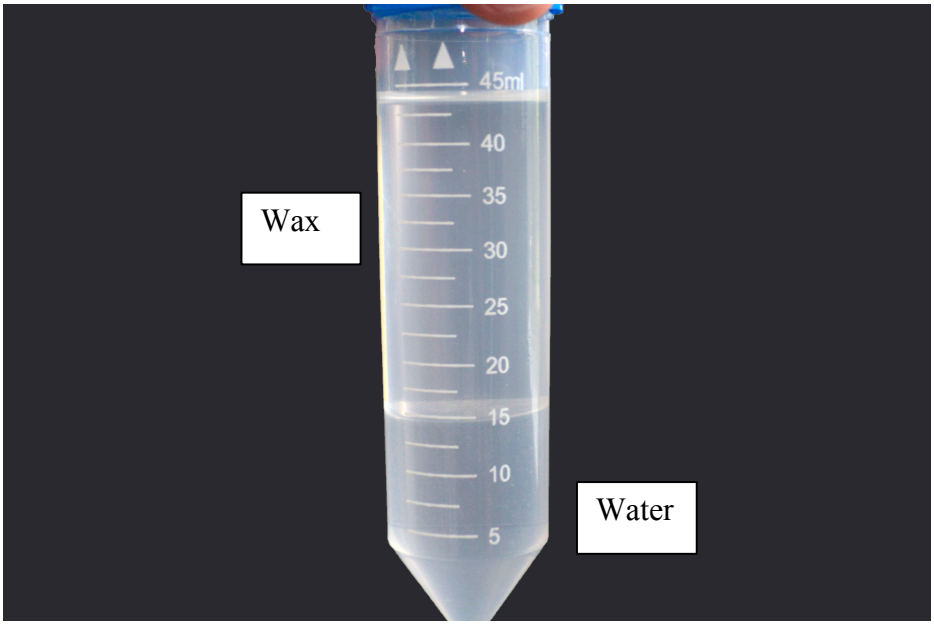

Figure 40 - Macrocrystalline Wax from Bottle #3

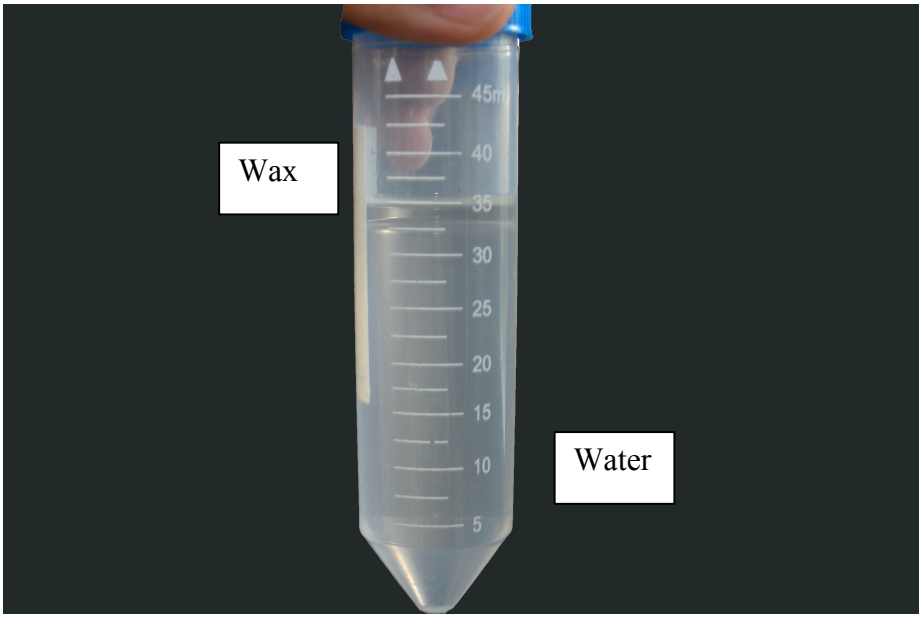

Figure 41 - Macrocrystalline Wax from Bottle #4

xi. Synthetic Microcrystalline Wax (Mixed at 9,000RPM, 75°C)

The synthetic microcrystalline wax managed to be poured from the beaker to the respective bottles for the bottle test before it separated. There were only negligible differences in volume after 30 minutes into the bottle test. Therefore, after 30 minutes of conducting the bottle test, it was concluded that the mixture has been fully separated.

Later on in the experiment, it was seen that the wax layer had reduced, as seen in Figure 42 below. This was witnessed on the third day onwards for all bottles.

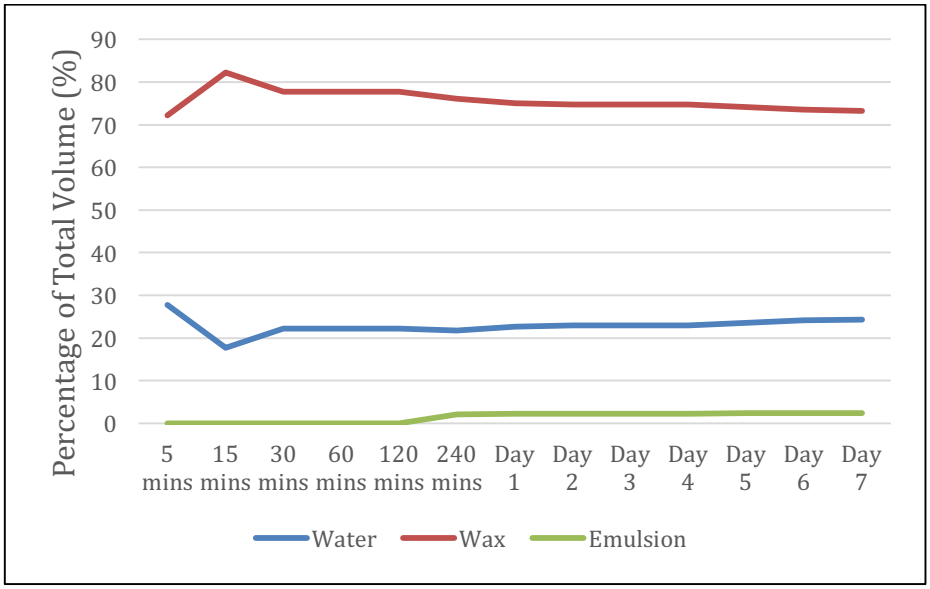

Figure 42 - Bottle Test Results for Microcrystalline Wax

A thin white layer was visible at the 240th minute of the experiment between the wax and the water layer. It is suspected that the rag layer for the microcrystalline wax formed at that time. This is recorded in Figure 43 and 44 below.

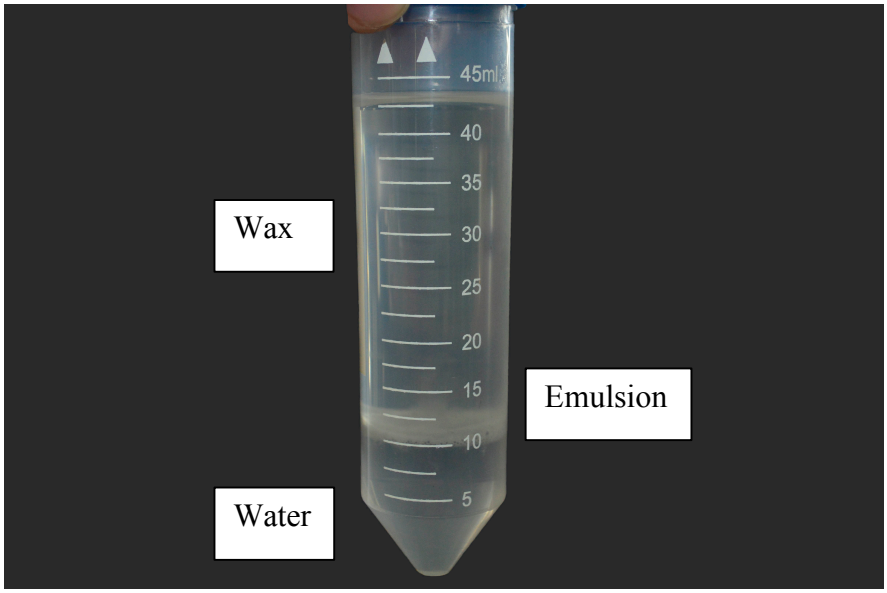

Figure 43 - Separation in Microcrystalline Wax Bottle #3

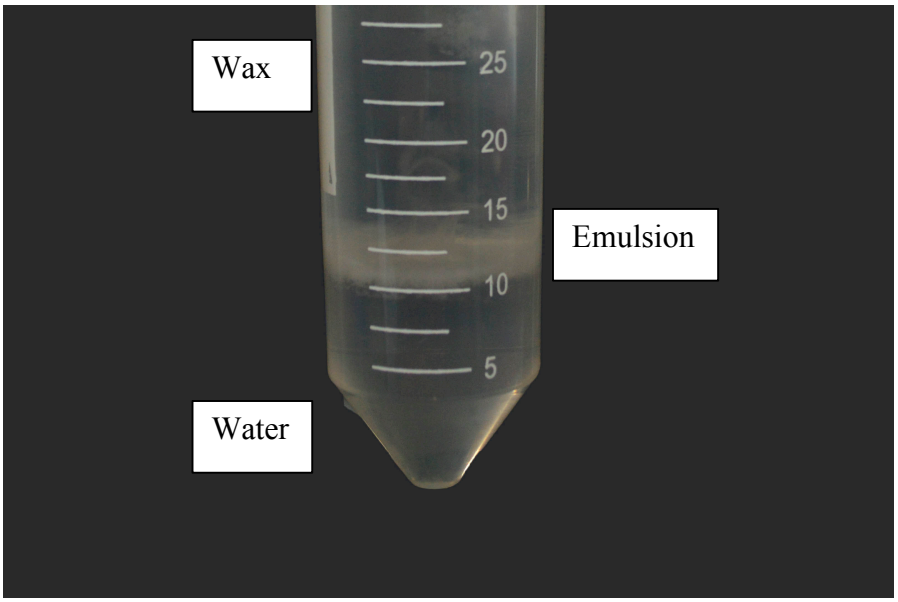

Figure 44 - Rag Layer Formed in Microcrystalline Wax Bottle #2

4.6. Rag Layer Microscopy

A sample of the rag layer of each samples was placed under the microscope to observe the composition of the materials inside the rag layer. This is to identify characteristics such as the type of emulsion produced, solid residues and the size of the bubbles inside the rag layer.

Observation was done on only three samples: A, B, and microcrystalline wax. Macrocrystalline wax was not observed due to the absence of rag layer.

i. Sample A

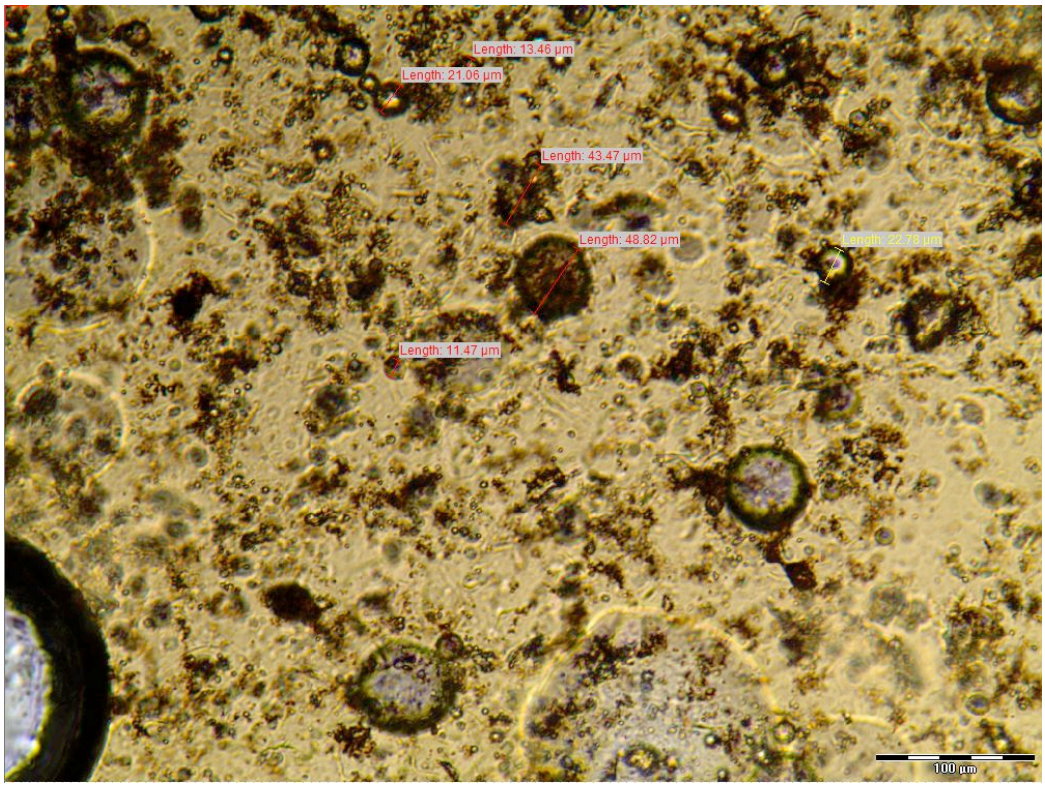

Figure 45 - Rag Layer for Sample A

The rag layer of Sample A consist mainly of oil-in-water emulsion with traces of solid particles surrounding the rag layer. This is observed through the presence of dark solid particles as seen in Figure 45. The oil bubble has an average size of 31.6 microns.

ii. Sample B

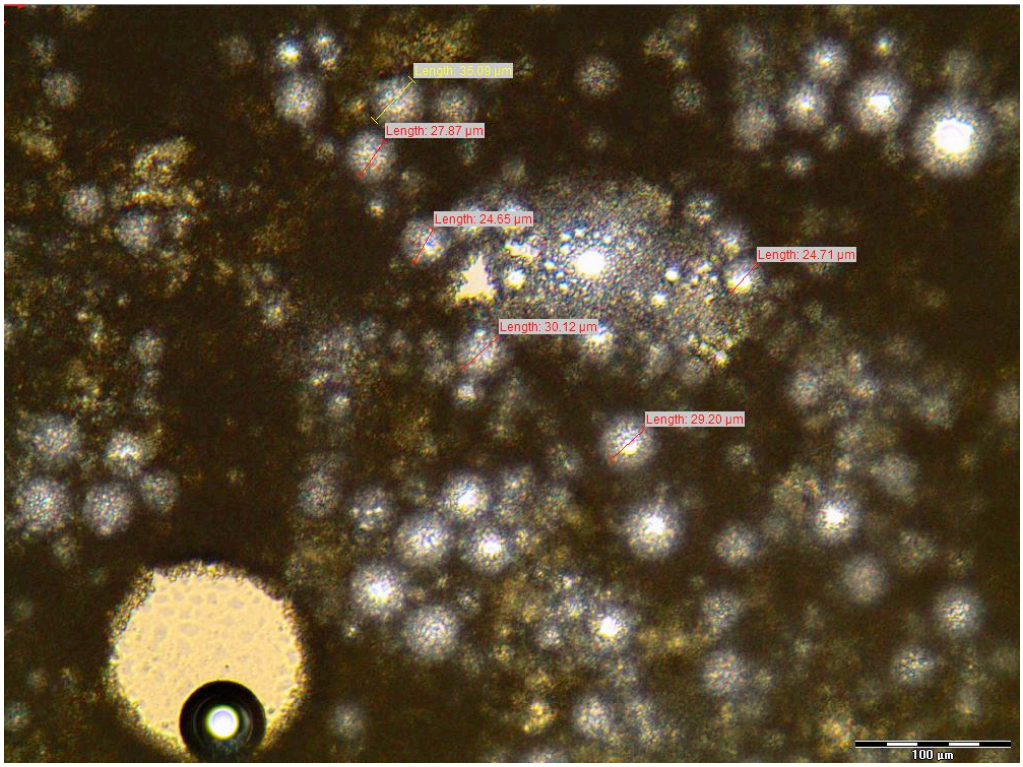

Figure 46 - Rag Layer for Sample B

Sample B mainly consist of a water-in-oil emulsion due to the overwhelming presence of oil in the rag layer. The average size of the water bubbles in the rag layer is found to be 28.6 microns

The presence of solid particles is not very visible when observed in Figure 46. However, based on the observation made from the bottle test, it is found that the Sample B rag layer has a thick layer of solid particles.

iii. Synthetic Microcrystalline Wax

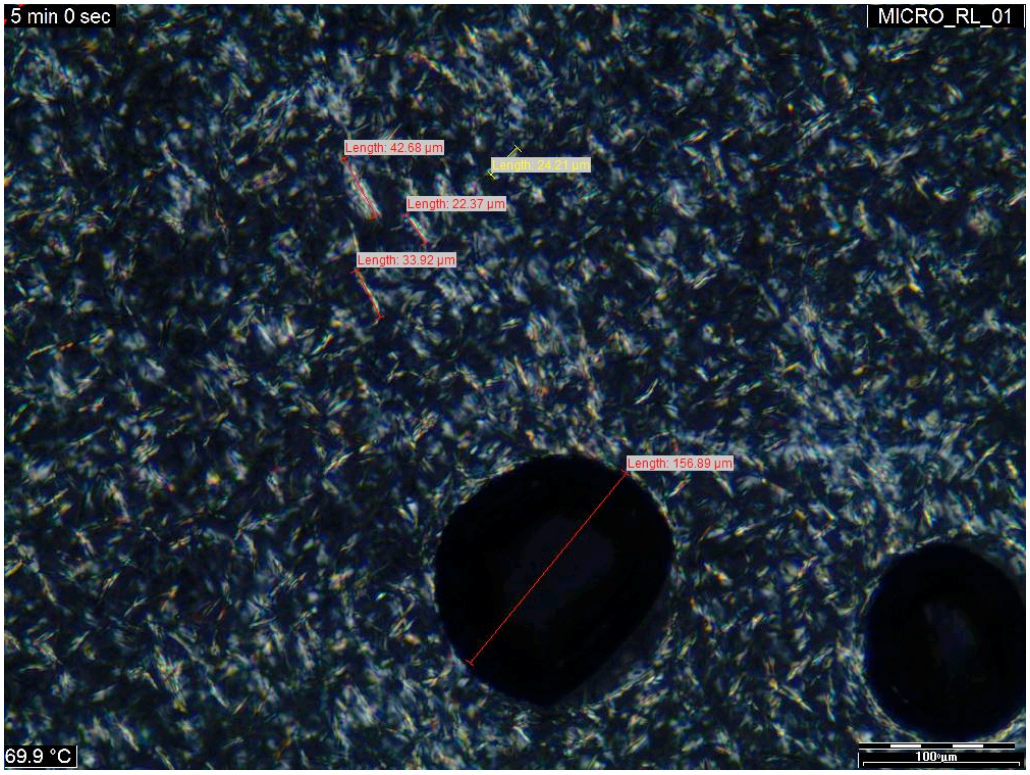

Figure 47 - Rag Layer for Synthetic Microcrystalline Wax

The rag layer microscopy for the synthetic microcrystalline wax is conducted under cross-polarized filter due to the transparent nature of the wax. It was observed that at 70°C, the wax has an average size of 30.8 microns.

However, it should be noted that the synthetic microcrystalline wax gels up at a high temperature (65°C). Therefore, the extraction of the rag layer was difficult, although the author tries as best to extract the rag layer and put it under microscopy. This was unlike the rag layer for Sample A and B, where it was easily extracted.

4.7. Water Content

The water content is recorded by using the V30 Compact Volumetric KF Titrator by Mettler Toledo. It can record water content from a minimum of 0.01% to 100% water content.

The samples are taken from the centrifuge bottle after the bottle test is completed. Three different samples are taken from the centrifuge bottle at different layers, which are the oil/wax layer, rag layer and the water layer.

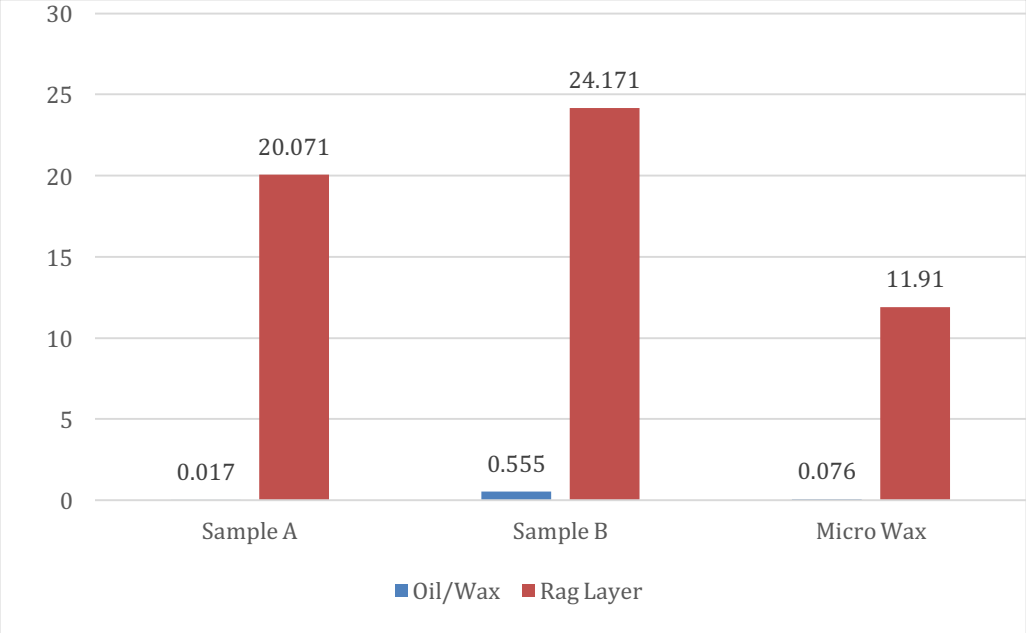

Figure 48 - Comparison of Water Content in All Samples in Percentage

As observed in Figure 48, except Sample B at 0.555%, the content of water in the pure oil and wax layer in taken from the centrifuge bottles are less than 0.5%, which is the export requirement for crude oil. The water content present in the rag layers are 20.071% for Sample A, 24.171% for Sample B and 11.91% for the synthetic microcrystalline wax.

The water content percentage for the water layer of the samples were not recorded as the results were not accurate.

CHAPTER 5

CONCLUSION AND RECOMMENDATION

4.1 Conclusion

In conclusion, the characteristics of the rag layers produced by the two different crudes, Sample A and B, and the synthetic microcrystalline wax was recorded. However, the synthetic macrocrystalline wax is not characterized as it did not produce any rag layer at the end of the bottle test.

Mechanical analytical methods were used to characterize the rag layers of all samples. Equipment such as rheometer, pour point tester, differential scanning calorimetry, cross-polar microscope, and titrator were used in the process, in addition to the bottle test, which was done manually.

The observations recorded in the experiment was that the actual crude oil produced rag layer of up to 10% of the total liquid volume. The macro wax produced unstable emulsion, resulting in no rag layer but the micro wax sample produced up to 2% - 3% rag layer. Therefore, the role of micro wax in the formation of rag layer is confirmed. More analysis needs to be done on the role of macro wax in rag layer formation.

4.2 Recommendation

The studies conducted can be expanded to include other crude oils in Malaysia so that comprehensive research can be done on the characteristics of rag layer in the crude oils of this region. While the experiments suggested were all based on mechanical tests, there were also chemical tests that could be conducted. However, the use of chemicals may complicate the process of understanding the rag layer as a whole due to the complexity of the chemicals used.

The effects of asphaltene, resins and other fine solids on the formation and characteristics of the rag layer could also be assessed individually. The influence of slip velocity between the phases as experienced in the separator on the formation of rag layer could also be explored as compared to the static bottle tests.

In addition to that, the use of artificially produced water might not be at par with those found in the same field as the composition of the produced water is unique to a field. Therefore, it may be important, whenever possible, to replicate a solution that is as similar to the produced water in the field on which the crude oil was found.

REFERENCES

Berridge, S.A., Dean, R.A., Fallows, R.G., Fish, A., 1968. The properties of persistent oils at sea. *J. Instit. of Petr.,* 300–309.

Fingas, M., & Fieldhouse, B. (2009). Studies on crude oil and petroleum product emulsions: Water resolution and rheology. *Colloids and Surfaces A-physicochemical and Engineering Aspects*, *2009*(333), 67-81. doi:10.1016/j.colsurfa.2008.09.029

Fingas, M., & Fieldhouse, B. (2012). Studies on water-in-oil products from crude oils and petroleum products. *Marine Pollution Bulletin*, (65), 272-283.

Goual, L. (2012). Petroleum Asphaltenes. In *Crude Oil Emulsions- Composition Stability and Characterization, Prof. Manar El-Sayed Abdul-Raouf (Ed.)*. doi:10.5772/35875

Jiao, J., & Burgess, D. J. (2003). Ostwald ripening of water-in-hydrocarbon emulsions. *Journal of Colloid and Interface Science*, *2003*(264), 509?516. doi:10.1016/S0021-9797(03)00276-5

Kiran, S. K., Acosta, E. J., & Moran, K. (2009). Study of Solvent?Bitumen?Water Rag Layers. *Energy & Fuels*, *23*, 3139-3149. doi:10.1021/ef8008597

Madjlessikupai, M. A., Harbottle, D., Masliyah, J., & Xu, Z. (2012). *Characterizing rag-forming solid*. Retrieved from http://www.ualberta.ca/CMENG/xumaster/files/Oil%20Sands%202012%20Conference%20Presentations/Morvarid%20Madjlessikupai%20-%20%20Copy.pdf

Madjlessikupai, M. A. (2012). *Study of the Rag Layer: Characterization of Solids* (Master's thesis, University of Alberta, Alberta, Canada).

Manar El-Sayed Abdel-Raouf (2012). Factors Affecting the Stability of Crude Oil Emulsions, *Crude Oil Emulsions- Composition Stability and Characterization, Prof. Manar El-Sayed Abdul-Raouf (Ed.)*, ISBN: 978-953-51-0220-5, InTech, DOI: 10.5772/35018. Available from: http://www.intechopen.com/books/crude-oil-emulsions-composition-stability-and-characterization/factors-affecting-the-stability-of-crude-oil-emulsions

Neto, A. A., Gomes E., A. S., Barros Neto, E. L., Dantas T., N. C., & Moura C. P., A. M. (2009). Determination of Wax Appearance Temperature (WAT) in Paraffin/Solvent Systems by Photoelectric Signal and Viscosimetry. *Brazilian Journal of Petroleum and Gas*, *3*(4), 149-157.

Particle Sizing System. (2012). Ostwald Ripening. Retrieved from pssnicomp.com/definitions/ostwald-ripening/

Pedersen, K. S., & Rønningsen, H. P. (2003). Influence of Wax Inhibitors on Wax Appearance Temperature, Pour Point, and Viscosity of Waxy Crude Oils. *Energy & Fuels*, *2003*(17), 321-328. doi:10.1021/ef020142+

PetroWiki. (n.d.). Oil demulsification. Retrieved October 10, 2014, from http://petrowiki.org/Oil_demulsification#Mechanisms_involved_in_demulsification

PetroWiki. (n.d.). Oil demulsifier selection and optimization. Retrieved October 10, 2014, from http://petrowiki.org/Oil_demulsifier_selection_and_optimization

PetroWiki. (n.d.). Stability of oil emulsion. Retrieved October 9, 2014, from http://petrowiki.org/Stability_of_oil_emulsions

PSL Systemtechnik. (1999). Background knowledge. Retrieved from http://www.psl-systemtechnik.de/pour_point_tester_knowledge.html?&L=1

Robins, M. M. (2000). Emulsions - Creaming Phenomena. *Colloid & Interface Science*, *2000*(5), 265-272.

Saadatmand, M., Yarranton, H. W., & Moran, K. (2008). Rag Layers in Oil Sand Froths. *Industrial & Engineering Chemistry Research*, *47*, 8828-8839. doi:10.1021/ie800601r

Silset, A. (2008). *Emulsions (w/o and o/w) of Heavy Crude Oils. Characterization, Stabilization, Destabilization and Produced Water Quality* (Doctoral dissertation, Norwegian University of Science and Technology, Trondheim, Norway). Retrieved from http://www.diva-portal.org/smash/get/diva2:127628/FULLTEXT02

Varadaraj, R., & Brons, C. (2007). Molecular Origins of Crude Oil Interfacial Activity Part 3: Characterization of the Complex Fluid Rag Layer Formed at Crude Oil?Water Interfaces. *Energy & Fuels*, *21*, 1617-1621. doi:10.1021/ef0606299

Wabel, C. (1998, July 30). Influence of Lecithin on Structure and Stability of Parenteral Fat Emulsions - Chapter 1 - Introduction. Retrieved from http://www2.chemie.uni-

erlangen.de/services/dissonline/data/dissertation/Christoph_Wabel/html/Chapter1.html

APPENDICES

1. Gantt Chart

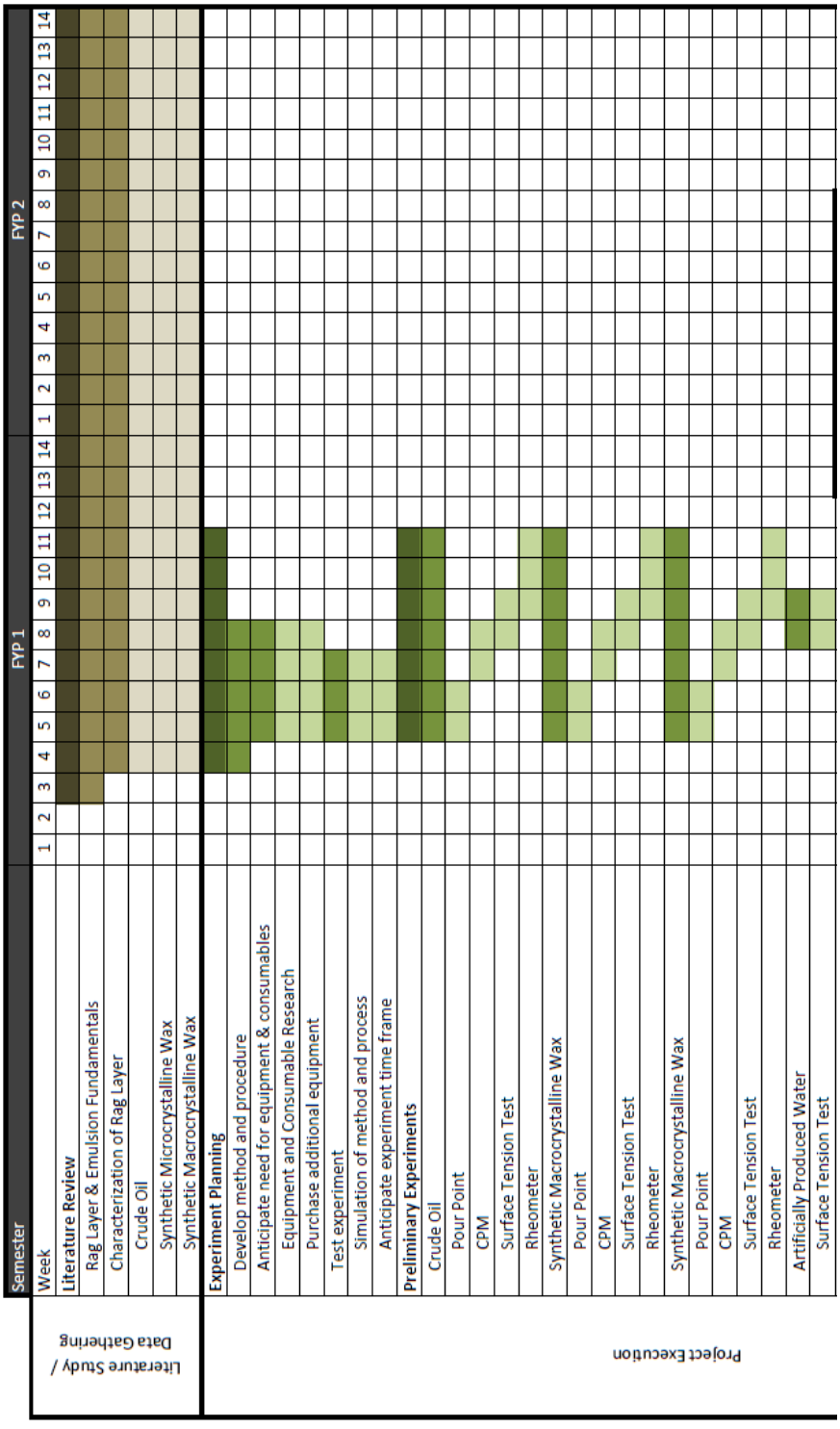

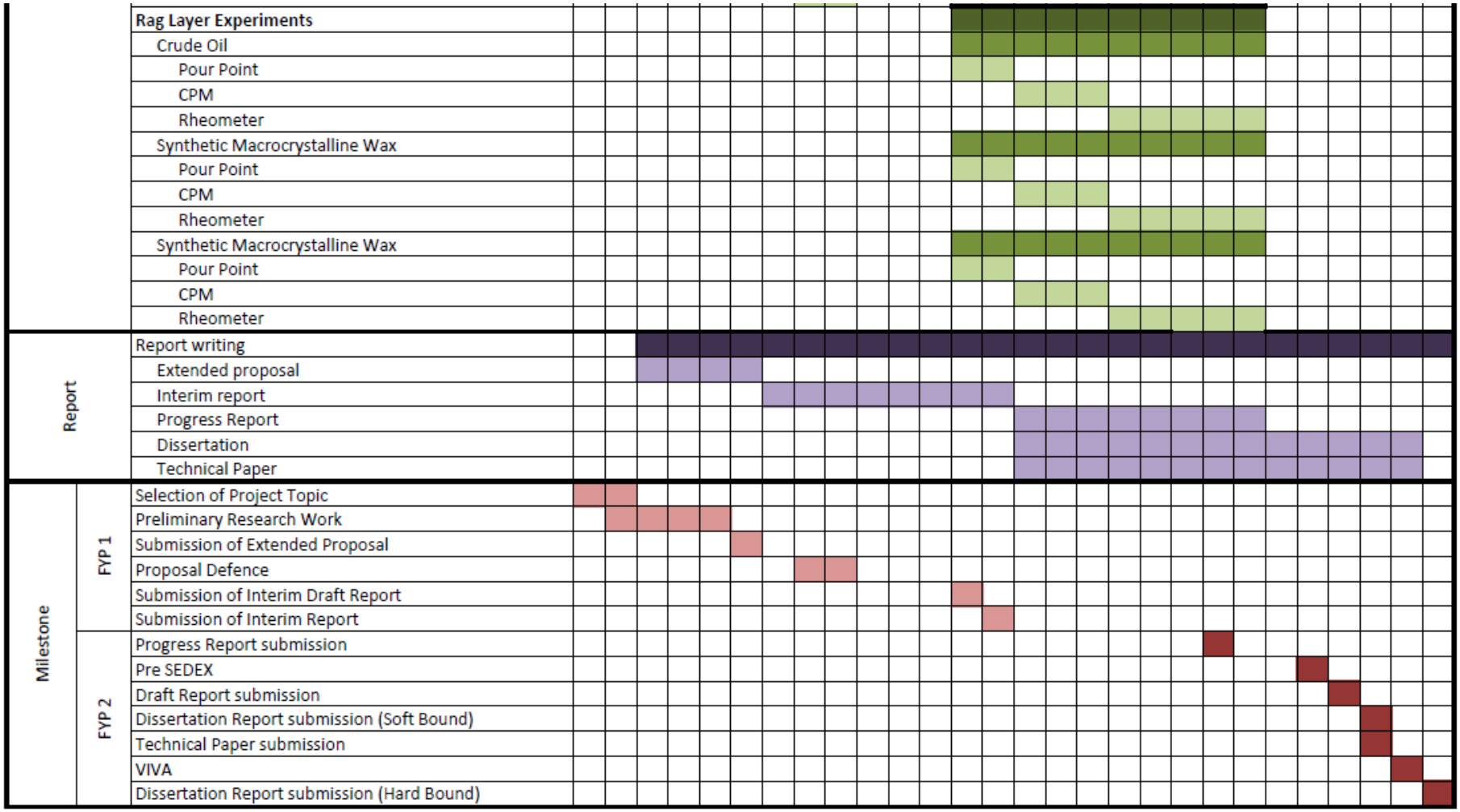
Rag Layer Experiments
Crude Oil
Pour Point
CPM
Rheometer
Synthetic Macrocrystalline Wax
Pour Point
CPM
Rheometer
Synthetic Macrocrystalline Wax
Pour Point
CPM
Rheometer
Report
Report writing
Extended proposal
Interim report
Progress Report
Dissertation
Technical Paper
Milestone
FYP 1
Selection of Project Topic
Preliminary Research Work
Submission of Extended Proposal
Proposal Defence
Submission of Interim Draft Report
Submission of Interim Report
FYP 2
Progress Report submission
Pre SEDEX
Draft Report submission
Dissertation Report submission (Soft Bound)
Technical Paper submission
VIVA
Dissertation Report submission (Hard Bound)

2. **Cross Polarized Microscopy**

Sample A – 12.5°C

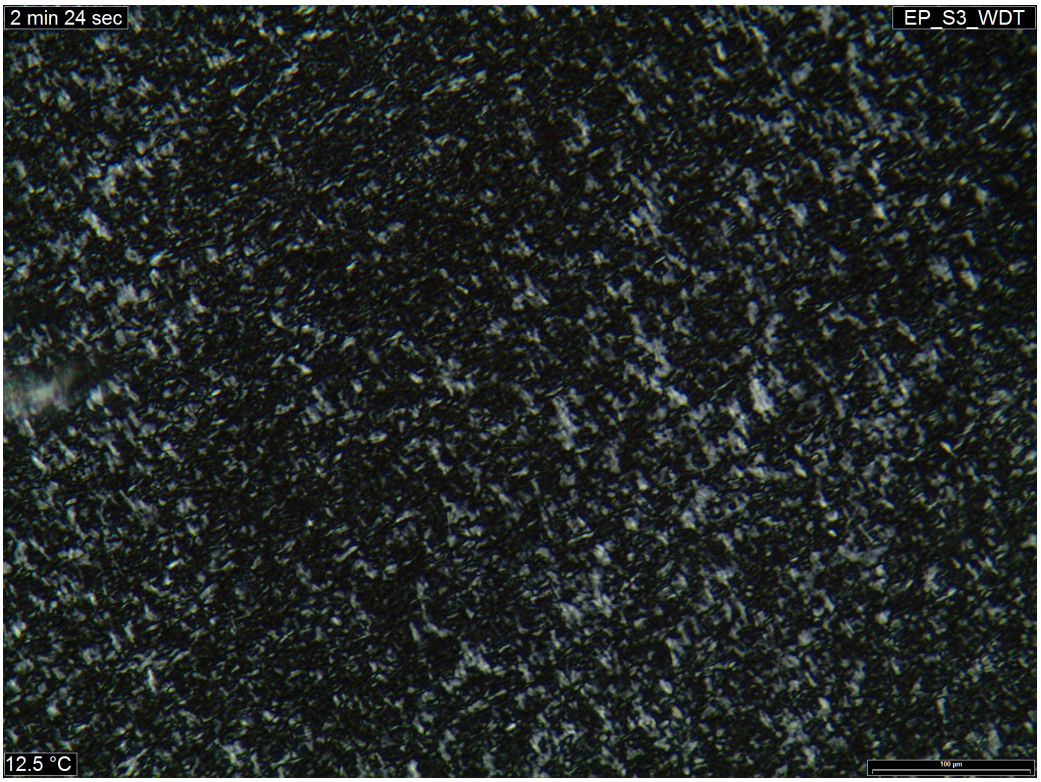

Sample B – 5.0°C

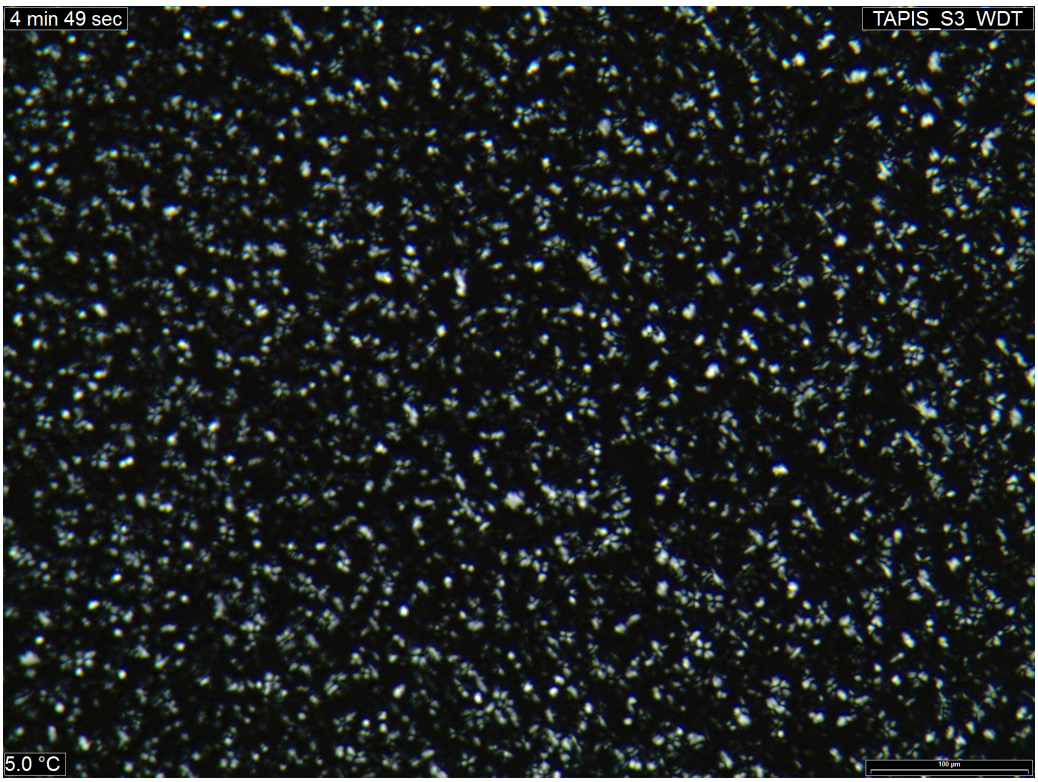

Macrocrystalline Wax – 25.1°C

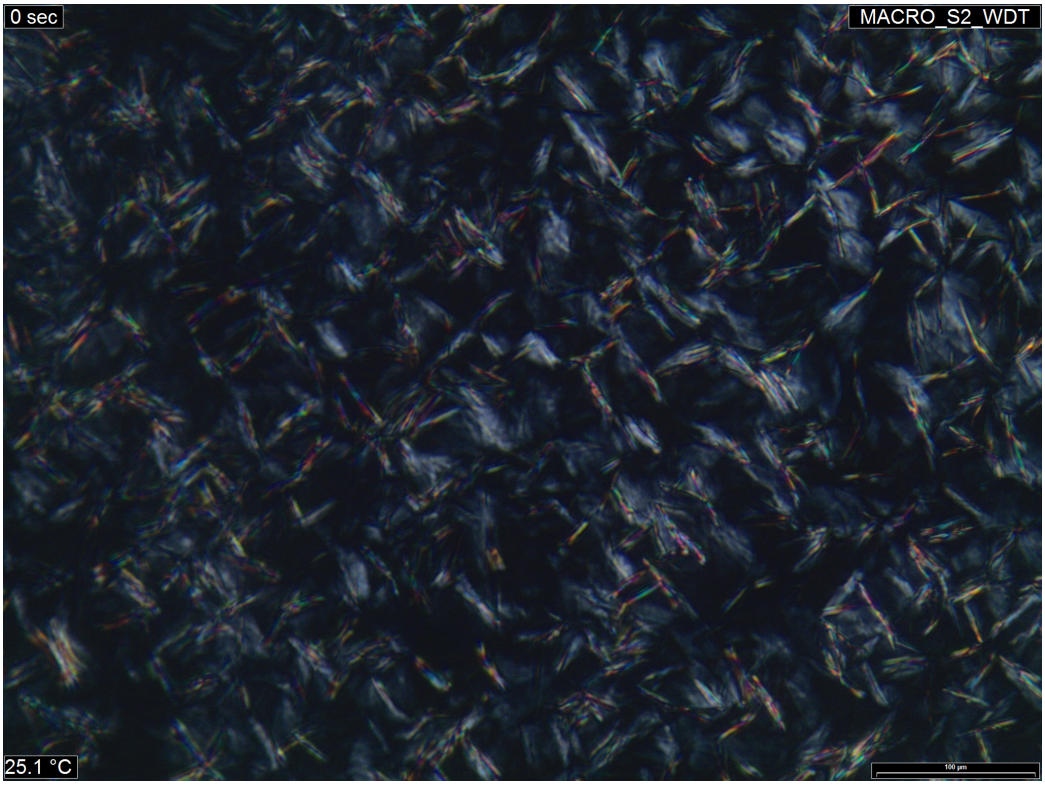

Microcrystalline Wax – 45.1°C